DUPLICATE ALSO

Forecasting Research

Met O 11 Technical Note No.15

Sensitivity of a medium range forecast with the Analysis Correction Scheme to data selection in the horizontal

by

B.Macpherson
and
R.Downton

November 1989

ORGS UKMO M
26 FEB 1990
Meteorological Library
FHQA 155669
National Meteorological Library
FitzRoy Road, Exeter, Devon. EX1 3PB

Meteorological Office (Met O 11)
London Road, Bracknell, Berkshire RG12 2SZ, England

LONDON, METEOROLOGICAL OFFICE.
Met.O.11 Technical Note (New Series) No.15

Sensitivity of a medium range forecast with the analysis correction scheme to data selection in the horizontal.

00180390 551.509.333

MET O 11 TECHNICAL NOTE NO 15

Sensitivity of a medium range forecast with the Analysis Correction scheme to data selection in the horizontal

by

B Macpherson

and

R Downton

November 1989

Met O 11
Meteorological Office
London Road
Bracknell
Berkshire, England.

Note: This paper has not been published. Permission to quote from it must be obtained from the Assistant Director of the above Meteorological Office Branch.

1. INTRODUCTION

The Analysis Correction (AC) scheme *(Lorenc, Bell and Macpherson, 1989)* underwent an operational trial in December 1987. As reported by *Bell (1988)*, many of the results from that trial were encouraging relative to earlier trials. This was true of wind errors in particular but also of other fields in the early stages of the forecast. During this period, however, the AC run produced two 5-day forecasts which were significantly worse than the operational product in the Atlantic sector. It is interesting that on both these occasions the ECMWF forecast was also inferior to the operational one. Our investigation concerns the case with largest forecast differences near the UK, data time 12 GMT on Boxing Day, 26/12/87.

We begin by summarising the synoptic background and the forecasts made at the time. Following this a number of sensitivity studies are described in Section 4. Experiments with data transplants between analyses were designed to locate regions of the analyses to which this medium range forecast was especially sensitive. Attention is then directed to the differences between operational and AC analyses in the sensitive areas. These are interpreted mainly in terms of the different observational influence areas in the two schemes, an interpretation supported by various AC assimilation experiments with reduced influence areas.

In Section 5 a data selection technique for the AC scheme is specified by making the influence area a function of data density. A comparison is presented with forecasts from assimilations with constant (large or small) influence areas. Drawbacks of the selection algorithm are explained and overall conclusions drawn in Section 6.

The global version of the AC scheme was implemented operationally on November 30th 1988. In this paper 'the operational (OP) scheme' refers to the system running before that date.

2. SYNOPTIC EVOLUTION

During the final week of December 1987 a succession of troughs and ridges embedded in the strong upper westerly flow moved quickly east across the Atlantic to western Europe. At 12 GMT on the 26th, the 500mb height field (Fig. 1(a)) showed vortices centred over Hudson Bay and the central Atlantic, with a very strong upper westerly flow extending from north-west Canada to the central USA. This flow then turned east along 40°N to the central Atlantic before returning north-east around the Atlantic vortex to the British Isles. A deep cut-off vortex was centred over the south-western USA, with a sharp upper trough at 140°W.

From the 26th to the 29th, changes in the upper flow over the Atlantic were relatively small as the vortex drifted slowly north-east towards Iceland and another centre took its place. Further west, the vortex over Hudson Bay moved south-east, whilst the low over the south-western USA moved east to form a deep trough over the eastern USA with a ridge developing on its forward side. During the next two days this low and trough system drifted east, with the ridge moving to 30°W. The low in mid-Atlantic combined with the low further north to form a deep trough at 5°W by the 31st (Fig. 2(a)).

Surface charts (Fig. 1(b)) showed a deep low moving north-east towards Iceland which later turned east to be centred just off north-west Scotland, as a secondary depression in association with the upper vortex moved east on its southern side. A shallow low in association with the upper vortex over the south-western USA moved east and deepened rapidly from 1013mb on the 28th to 960mb by the 30th. It reached the Atlantic to be just north-east of Newfoundland by the 31st (Fig. 2(b)).

3. FORECASTS FROM DATA TIME 12 GMT, 26/12/87

Figures 3, 4 and 5 show the OP, AC and ECMWF 5-day forecasts, to be compared with the verifying analysis for 12 GMT on the 31st (Fig. 2). Clearly, the OP forecast is the best of the three. By t+72 the AC run verifying at 12 GMT on the 29th had produced a significantly better depth for the surface low at 37°N, 40°W than the OP forecast *(Bell, 1988)*, but the AC forecast was worse by that stage over the USA, where the upper ridge at 100°W was too flat and the trough near 80°W too shallow. This lack of amplitude became more apparent during days 4 and 5 as the forecast upper flow betweeen 40-55°N over the Atlantic became very zonal and the upper lows further to the north moved too quickly eastwards. The greater amplitude in the ridge at 100°W from the OP t+72 forecast led to the production of a stronger northerly flow into the rear of the trough at 80°W. This had the effect of slowing down the eastward movement of the trough, allowing a ridge to develop in mid-Atlantic and the forward trough to sharpen as it reached the British Isles by day 5.

4. SENSITIVITY STUDIES

4.1 Data Transplants

The significant differences over the USA between the forecasts by day 3 appeared to develop from analysis differences over the western USA and Pacific (Fig. 6). Figure 7 shows the difference between the OP and AC runs by t+120. To evaluate the significance of the t+4 differences, analysis data for all 15 model levels and for various areas over the USA and the Pacific were transplanted from the OP t+4 forecast into the AC analysis.

The transplant area giving the most successful forecast extended from (20-70°N, 90-140°W). This area covered the upper low over the south-western USA and the trough over the east Pacific. By t+120 there was a noticeable improvement in the forecast over the Atlantic, with a slight improvement over the UK and Western Europe. Figure 8 shows the difference by t+120 between the AC run with the OP transplant and the first AC run with no transplant. The correspondence with Figure 7 is striking.

Transplants of smaller areas giving less successful impact (Figs. 9 and 10), highlight the importance of particular areas in the most successful run. Comparing Figure 9 with Figure 8, we deduce that the region 90-120°W over continental America brought significant impact, but that the contribution from 120-140°W was also appreciable, as confirmed more directly by Figure 10 (with a 10° westward extension of the transplant area). The AC phase error represented by the difference maxima near the UK and Scandinavia in Figure 7 is best explained by those transplants including the region 120-140°W (Figs. 8 and 10). The west Atlantic maxima in Figure 7 appear to originate about equally from analysis differences in the sectors 90-120°W and 120-150°W. A transplant of the mid and west Pacific (not shown) was less helpful but suggested a connection with the west Atlantic feature. The eastern USA was determined by another transplant not to be relevant to the 5-day differences.

Having identified a region within which analysis differences were important for the differences between forecasts, we now describe these differences in more detail.

4.2 Analysis differences

Since assimilation of asynoptic data in the AC scheme is only completed at t+4, we present fields for this time within the area identified by the transplant experiments.

At 250mb, the OP run has more ridging than the AC analysis to the west and east of the low in the south western USA (Fig. 11). The isotachs (Fig. 12) show a stronger jet in the AC analysis over northern Mexico and differences in the jet entrance region to the west. A stronger jet relative to the OP run is uncharacteristic of the AC scheme. The OP jet over Vancouver is stronger than the AC one. We can summarise Figures 11 and 12 by saying that the OP and AC analyses gave different treatments of the flow branching at the base of the east Pacific trough. The OP solution took more of the flow north towards Canada whereas in the AC run more was diverted south round the low. This behaviour is also evident from the pattern of maxima and minima in the 250mb height field (Fig. 13). We now describe experiments to shed light on the origin of these differences.

4.3 Reduced influence area in the AC scheme

The OP scheme gives data a smaller influence area than the AC scheme. The importance of this for the 5-day forecast was tested in three experiments. In each, four AC assimilation cycles were repeated with a reduced influence area for certain data: in the first for radiosondes only (Fig. 14), in the second for aireps and satobs (Fig. 15) and in the third for all data (Fig. 19).

a *For radiosondes*

In Figure 14 we see a much smaller phase error in the western upper vortex (comparing with Fig. 4) and only one associated surface low, though it is still too fast. The phase error in the UK surface low is slightly worse. Relative to the original AC run, a reduction of the influence area for radiosondes raised analysed heights to the east of the low over south-western USA (Fig. 16). The OP run (Fig. 13) also had higher heights in this area, so this difference in the experiment may be responsible for the improvement in the west Atlantic at day 5. Some of the locations of radiosonde data in areas of largest height difference are marked in

Figure 16. The differences south of 45°N are in a relatively data rich area where the reduced influence area has produced a better fit to observations. The differences in Figure 16 are most unlike those in Figure 13 to the west of Hudson Bay and this less data rich area could be linked with the poorer treatment of the UK low in the experiment.

b For aireps and satobs

The experiment with a smaller influence area for these single level wind data (Fig. 15) held back and deepened the forecast low over the UK by 10mb, a significant improvement on Figure 4. The phase error in the west Atlantic upper vortex was, however, increased. The analysed height differences (Fig. 17) are large off the west coast of Mexico and California, as are those for the OP scheme (Fig. 13). The jet core over northern Mexico (Fig. 18) has shrunk relative to the first AC run (Fig. 12(b)) and has a smaller peak wind speed. In relation to the airep and satob locations for the last assimilation cycle, these differences lie downstream. It is known *(Barwell and Lorenc, 1985)* that repeated insertion can generate excessive wind maxima downstream of observations. It is possible that this occured in the original AC run and was alleviated by the smaller influence area in the experiment.

c For all data

This run (Fig. 19) puts the western vortex between the positions when either radiosondes or single level winds alone were affected. There was also a marginal improvement on Figure 15 for the UK low, perhaps due to the smaller influence area for surface data.

The question arises as to whether radiosonde temperatures or winds were more important for the west Atlantic vortex. The experiment was repeated with reduced weighting to geostrophic wind increments. The result (Fig. 20) was a much poorer phase for the west Atlantic vortex. As the geostrophic coupling is designed to aid assimilation of mass data, it appears that mass data, and in particular radiosonde temperatures, were important for the west Atlantic feature at day 5. The analysis differences between the experiments in Figures 19 and 20 (Fig. 21) show maxima to the east of the low, in an area already identified by Figure 16. The fit of analyses to radiosonde height data for the OP and original AC runs is compared in Figure 22. Some key data to the east of the vortex are less well fitted by the AC analysis - this is consistent with the reduced influence area difference maps in Figures 16 and 21.

5. DATA DENSITY DEPENDENT DATA SELECTION IN THE AC SCHEME

5.1 Motivation

The experiments with reduced influence area have shown that a large influence area for some observations can degrade a medium range forecast. The sensitive regions in this case are characterised by relatively high data density. On the other hand, earlier work with the AC scheme has shown a clear improvement from the larger influence area in data sparse regions. The natural question arising is whether the AC scheme can be modified to retain a large influence area in data sparse regions, while permitting a smaller one where data density is high.

The OP scheme has such a variable influence radius because it allows a maximum of 7 influencing observations per grid point - the maximum radius is much smaller than the constant radius of the AC scheme. In the AC analysis of wind data for 12 GMT, 26/12/87 (Fig. 23), some grid points have up to 90 influencing observations near 140°W and most of the central USA has values in the range 20-30. By contrast, the run with constant small influence area (Fig. 24), giving a better forecast, has a maximum of 15 and most of the USA grid points are influenced by less than 5 data. For a more generally applicable variable influence area scheme, a minimum of around 10 data per grid point would seem reasonable.

The data selection algorithm of the OP scheme *(Bell and Dickinson, 1987)* takes account of data type as well as data density, with the ability to select radiosondes in preference, say, to satellite data that may be nearer the grid point. This is not possible in the AC scheme, in which the code is structured to loop over observations rather than grid points and there is no searching of observation lists for each grid point. The scheme derived and tested in the following sections is a function of data density, which is analysed by the scheme prior to the calculation of normalised observation weights. There is a slight implicit dependence on observational error (and hence type) through its entry into the data density calculations.

5.2 A test scheme - derivation

We consider the analysed increment $\Delta\mathbf{x}$ at the location of a group of $\mathbf{N}$ collocated data with equal errors. The AC scheme gives:

$$\Delta\mathbf{x} = \mathbf{Q'}\ \mathbf{R}^2 \sum_i C_i \tag{5.1}$$

where we assume that each observation has time factor $\mathbf{R}$ and C_i are the (observation - background) increments. The normalisation factor is

$$\mathbf{Q'} = (\varepsilon^2 + \mathbf{NR})^{-1} \tag{5.2}$$

where ε is the ratio of observation to background error and $\mathbf{NR}$ is the data density. The normalised weight for each observation is

$$\mathbf{W} = \mathbf{Q'}\ \mathbf{R} = \mathbf{R} / (\varepsilon^2 + \mathbf{NR}) \tag{5.3}$$

The normalised weight is defined as $\mathbf{Q'}\ \mathbf{R}$ rather than $\mathbf{Q'}\ \mathbf{R}^2$ because one power of $\mathbf{R}$ is removed as a temporal correlation in the same way that the spatial correlation has been suppressed in (5.1) by focussing on the increment analysed at the observation point instead of the grid point.

The proposed variable influence area scheme leaves the area A_B unchanged for a single isolated observation ($N=1$) but reduces it in a data rich area (large N) according to the ratio of the datum's actual normalised weight to the one it would have if it were isolated. The new area A_A is then

$$A_A \;/\; A_B \;=\; Q' \, R \,\left(R/[\varepsilon^2+R]\right)^{-1} \;=\; Q' \,(\varepsilon^2+R) \qquad (5.4)$$

For the example situation,

$$A_A \;/\; A_B = \left(\varepsilon^2+R\right) \;/\; \left(\varepsilon^2+NR\right) \qquad (5.5)$$

For N large there is only a weak dependence on ε and R as the reduction factor tends to N^{-1}. From such a scheme we of course expect

$$\left(A_A \;/\; A_B\right)_i \approx \left(N_A \;/\; N_B\right)_k \qquad (5.6)$$

where now N_B and N_A are the number of data influencing a grid point k in a data rich area before and after the influence areas of the observations i have been reduced. The scheme's impact on wind data (Fig. 25, compare with Fig. 23) gives $N_A/N_B \approx 0{\cdot}25$ in the most data dense areas and $N_A/N_B \approx 0{\cdot}5$ in central USA. Some complications arising in the application of (5.4) should be mentioned.

a Level independence

The influence radius in the AC scheme is independent of level but the normalisation factor Q' is not. Also, for single-level data the routine calculating influence radii receives values of

$$Q_{1M} = \varepsilon_L^{-2} \, \mu^v_{LM} \qquad (5.7)$$

rather than ε_L^2, where μ^v_{LM} is the vertical correlation between data level L and model level M. The value of ε^2 for (5.4) was therefore taken from (5.7) at the level of maximum Q_{1M}, as close as possible to the data level. For multi-level data, where ε_L varies with level, the level with maximum Q_{1M} was again taken to calculate ε^2 for (5.4).

The treatment of single-level data also determined the level from which the Q' values for (5.4) were selected. The vertical profile of Q' values is

$$Q_{2M} = Q'_L \, \mu^v_{LM} \qquad (5.8)$$

where Q'_L is the value at the data level. In order to base the new influence radius for single-level data on conditions at the data level, the maximum Q_{2M} value in the profile was chosen and this criterion was also applied to multi-level data.

b Renormalisation of weights

The Q' values in (5.4) are based on preliminary analysis of the data distribution employing a constant large influence area. The new smaller influence areas then lead to a smaller sum of normalised weights at each grid point (Figs. 26, 27). This represents a significant reduction in observational forcing relative to model background and, despite the smaller influence areas, early tests of the scheme produced analyses fitting the data less well than that with the constant larger area. The variable nature of this reduction in forcing ruled out a simple increase in relaxation coefficient as the cure and so a selective renormalisation of **Q'** values was devised as follows.

The sum of normalised weights at a grid point **k** is

$$S_k = \sum_i \mu_{ki} \, Q'_i \, R_i^2 \tag{5.9}$$

and we will assume that in a data rich area initially N_B observations influence grid point **k** from distances which give rise to an average correlation $\bar{\mu}_B$ for the group. When N_B is large, the normalisation factor Q'_i may be approximated by

$$Q'_{iB} = (N_B \, R \, \bar{\mu}_B)^{-1} \tag{5.10}$$

After application of (5.4), we have new values N_A and $\bar{\mu}_A$, with $\bar{\mu}_A > \bar{\mu}_B$ because the influence areas are smaller. The correct renormalised **Q'** value to conserve S_k in (5.9) is

$$Q'_{iA} = (N_A \, R \, \bar{\mu}_A)^{-1} \tag{5.11}$$

Rather than try to calculate N_A and $\bar{\mu}_A$ exactly, we propose a linear relationship of the form

$$Q'_A R = a \, Q'_B R + b \tag{5.12}$$

where **a** and **b** are constants to be selected so that two limiting cases are treated as correctly as possible. When $Q'_A = Q'_B$ (isolated single observation) there is no influence area reduction and (5.3) with **N**=1 gives

$$b \,/\, (1-a) = R \,/\, (\varepsilon^2+R) \tag{5.13}$$

When **N** becomes large, $\bar{\mu}_A \to 1$ as the new influence area reduction factor tends to N^{-1}. For uniform high data density and a large initial influence radius we can approximate $\bar{\mu}_B \simeq 0{\cdot}5$ and (5.4) with (5.10) and (5.11) give

$$1 = (\bar{\mu}_A Q'_A N_A) \,/\, (\bar{\mu}_B Q'_B N_B) \quad \to \quad 2 \, Q' \, (\varepsilon^2+R) \tag{5.14}$$

In (5.12) this case gives

$$b = R \,/\, (2 \, \{\varepsilon^2+R\}) \tag{5.15}$$

as $Q'_B R$ becomes negligible. The solution of (5.13) is now **a**=0·5, so that

$$Q'_A R = \{ \, Q'_B R + R/[\varepsilon^2+R] \, \} \,/\, 2 \tag{5.16}$$

from which we see that the renormalised weight is the average of the original normalised weight and the normalised weight for an isolated observation.

The effect of (5.16) is to restore higher values of S_k (compare Fig. 28 with Figs. 26 and 27), although by an excessive amount where the data density is highest, with S_k values as high as 3 instead of the theoretical maximum of 1.

Over much of the USA, however, renormalised S_k values are only about 20% larger than the original ones in Fig. 26 and this is better than being around 20% smaller as in Fig. 27 with reduced influence radii but no renormalisation. The larger S_k values contribute to the objective of a closer fit to observations, although it is mainly the smaller scale of the analysis increments from which we expect benefit.

A more rigorous renormalisation would involve recalculating the data density based on the new smaller influence areas and deriving new factors **Q'** from these. This option was rejected as impractical for general use as it would entail an increase in computation time for the analysis of approximately 50%.

5.3 <u>Test scheme - performance</u>

The variable influence area scheme produced the 5-day forecast in Fig. 29. The position of the western Atlantic 500mb vortex is better than the original trial run (Fig. 4) and as good as the run with constant small influence area (Fig. 19) but not as good as the run with reduced influence area only for radiosondes (Fig. 14). The surface low near the UK shows negligible improvement over the original run, is not as good as the run with constant small influence area or the run with reduced influence area for single-level wind data (Fig.15).

For an objective and more general measure of the scheme's performance, Table 1 compares the 5-day forecasts against radiosonde data for the whole northern hemisphere. We see that despite the apparent lack of surface impact in the Atlantic, the scheme does improve pmsl score over the trial run, though only by about half as much as the run with constant small influence area. In the height field, the fractional improvement relative to the AC trial run decays with height and in the temperature and wind fields, the variable area scheme cannot match the improvement of the constant small area run.

In case it might be thought generally desirable to have a constant small influence radius, Table 2 shows that results at t+24 are not as satisfactory. In particular the wind field verifies worse in the small influence area run than in either the original trial or variable area runs. Too much noise is generated by the small area for an acceptable short period forecast. Results for the southern hemisphere out to t+72 did not show any of the experiments to be consistently better than the original AC trial run. Also, the second case from the same operational trial period with a poor AC forecast was not improved by either the variable influence area scheme or the constant small area version.

			original AC trial	constant small influence area	variable influence area scheme
pmsl		(mb)	10·0	8·5	9·3
height -	850 mb	(dm)	6·9	5·7	6·4
	500		9·7	8·2	9·3
	250		12·8	11·1	12·2
temp -	850 mb	(K)	5·5	5·1	5·6
	500		4·3	3·9	4·2
	250		4·2	4·0	4·2
wind -	850 mb	(kts)	22	19	21
	500		32	28	32
	250		43	39	43

<u>Table 1</u>

Rms differences from verifying radiosondes in the northern hemisphere for three 5-day forecasts from different AC analyses

			original AC trial	constant small influence area	variable influence area scheme
pmsl		(mb)	3·2	3·2	3·2
height -	850 mb	(dm)	1·9	1·8	1·8
	500		2·7	2·8	2·7
	250		3·7	3·7	3·7
temp -	850 mb	(K)	2·7	2·9	2·8
	500		1·7	1·7	1·7
	250		2·5	2·5	2·5
wind -	850 mb	(kts)	10·7	10·9	10·8
	500		13·1	13·6	13·4
	250		15·6	16·3	15·5

<u>Table 2</u>

As Table 1 for the 24-hour forecasts

5.4 Problems and prospects

The results above show that it is possible to improve a particular medium-range forecast over a fairly wide area once its accuracy can be proved sensitive to the analysis in a small area. They also confirm the difficulty of deriving a simple data selection scheme that will give improved performances at all forecast times and on a global scale for all model variables in at least a majority of cases.

There are two main obstacles to a scheme of this kind. An accurate short-period forecast must start from a well balanced analysis. Excessive small scale detail, even that which may become important later in the forecast, is undesirable in the early stages. Secondly, a scheme which identifies small areas where the data density is high enough to warrant inclusion of smaller scales may be expensive, although the expense of weights renormalisation may be offset by the reduced cost of smaller influence areas in the regions identified. The rather *ad hoc* renormalisation of observational weights attempted above would have to be improved by a further data density analysis based on the revised influence areas calculated from the first step. One possible way forward would be to execute only one such sophisticated iteration per assimilation cycle. This would scan the data in space and time to calculate an appropriate influence radius for each observation to be used at every iteration of its insertion period. This prior analysis might also allow one to vary the insertion period with temporal data density and provide a better temporal component to the weights normalisation factor (*Lorenc, pers. comm.*).

6. CONCLUSIONS

The poorest forecast from the AC scheme's operational trial over Christmas 1987 was examined in detail. Transplants of data from the operational analysis, which gave a very good forecast, into the AC analysis revealed deficiencies in the AC analysis in the east Pacific and over south-western and central southern parts of the USA. Experiments with reduced observational influence area in the AC scheme showed that a closer fit to radiosonde temperature data over the southern USA led to a better 5-day forecast of the west Atlantic pattern and a closer fit to single-level wind data in the east Pacific improved the forecast pattern for the east Atlantic. A run with small influence area for all data types was better at day 5 than the original trial run but had a poorer wind field at t+24.

A simple scheme was proposed for data density dependence of the influence area in the AC scheme, which reduced the number of observations influencing each grid point by around one half to a quarter in the areas of interest over the USA. The 5-day forecast from this scheme verified better than the original trial run but not as well as the small influence area run. The 24-hour forecast of the wind field was better than the small influence area run. Renormalisation of the observation weights was a problem with this simple scheme, only partially overcome. The scheme did not improve the southern hemisphere forecast and did not correct an error in a second case from the trial. It is suggested that any scheme of this kind with more general applicability be incorporated in a once only four-dimensional analysis of data density performed prior to each assimilation cycle. The existence of the Boxing

Day case and others investigated by *Downton, Bromley and Ayles (1988)* supplies ample motivation for such work.

7. ACKNOWLEDGEMENTS

R.S. Bell provided diagnostics on forecast differences and D. Robinson assisted with objective verification.

8. REFERENCES

Barwell B.R. and A.C. Lorenc	1985	A study of the impact of aircraft wind observations on a large-scale analysis and numerical weather prediction system. Quart. J. R. Meteorol. Soc. 111, 103-129.
Bell R.S.	1988	A further global trial of the analysis correction scheme - Christmas 1987. Meteorological Office. Met O 11 Tech. Note No. 14.
Bell R.S. and A. Dickinson	1987	The Meteorological Office operational numerical weather prediction system. Sci. Pap. Meteorological Office, No. 41.
Downton R., Bromley R.A. and M.A. Ayles	1988	The 5-day forecast trial of the AC scheme. Meteorological Office, Met O 11 Tech. Note No. 12.
Lorenc A.C., Bell R.S. and B. Macpherson	1989	The new Meteorological Office data assimilation scheme. Meteorological Office, Met O 11 Tech. Note No. 27.

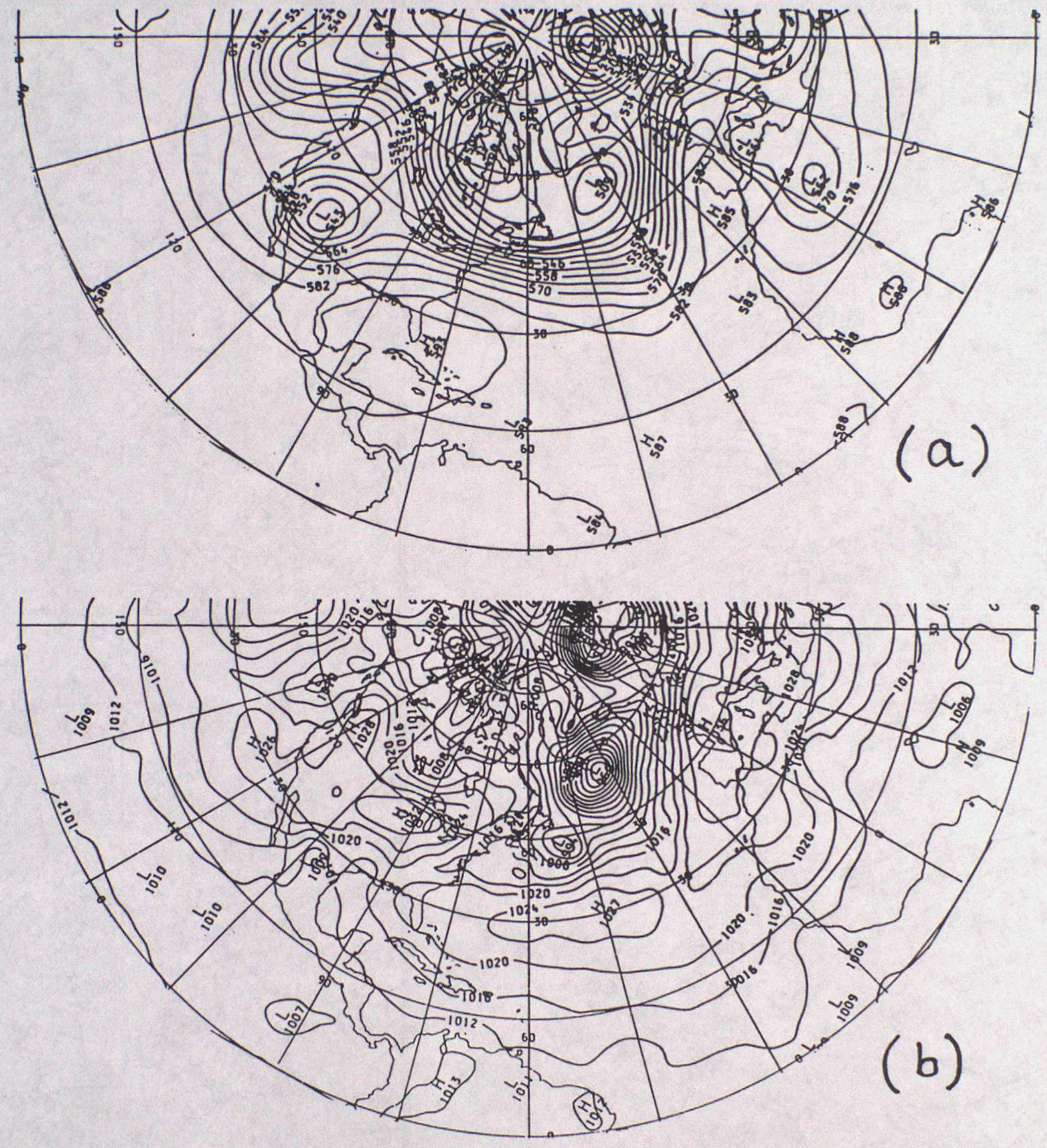

Figure 1 Operational analyses for 12 GMT, 26/12/87:
(a) 500 mb (b) surface

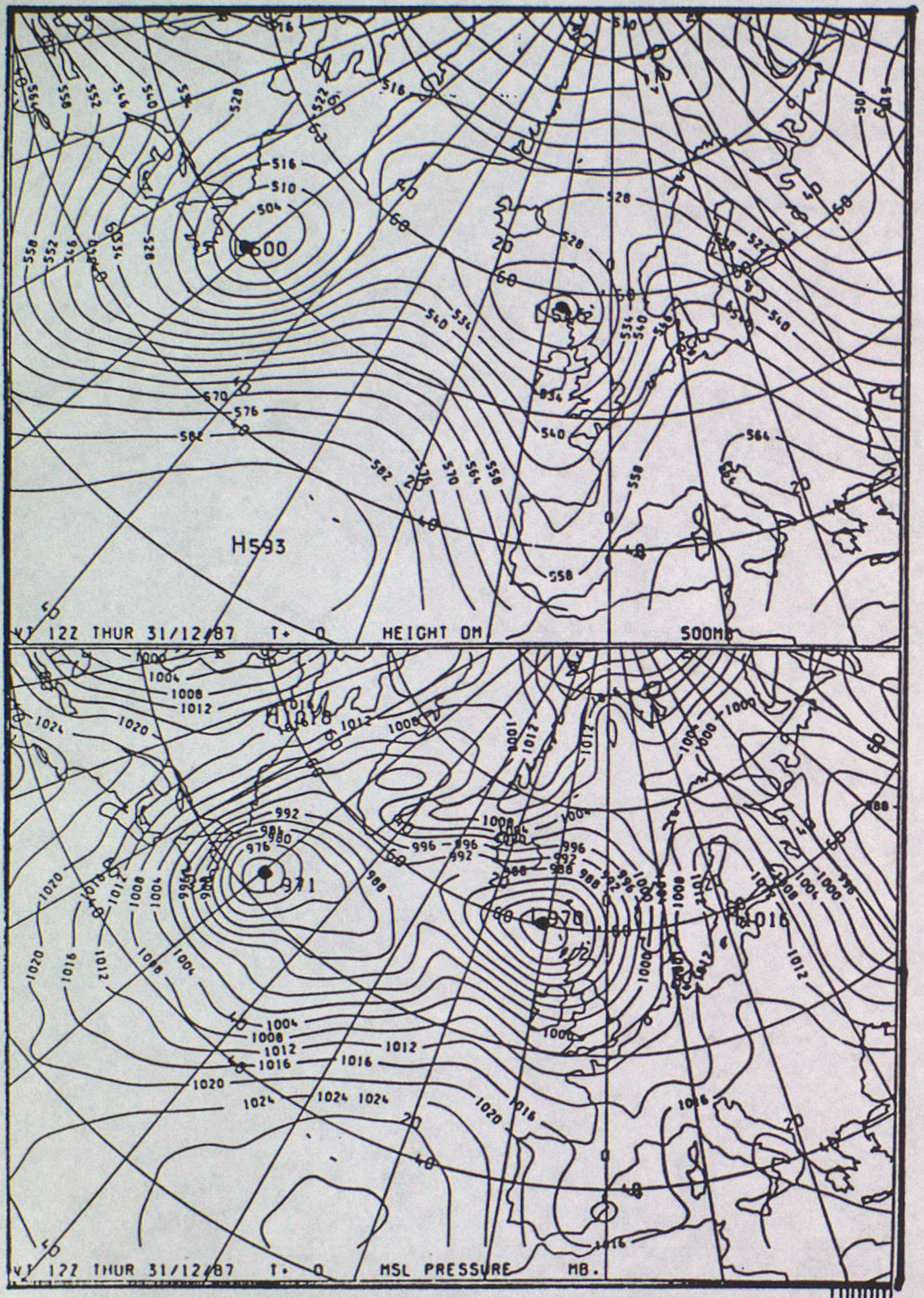

Figure 2 Operational analyses for 12 GMT, 31/12/87
(a) 500mb (b) surface

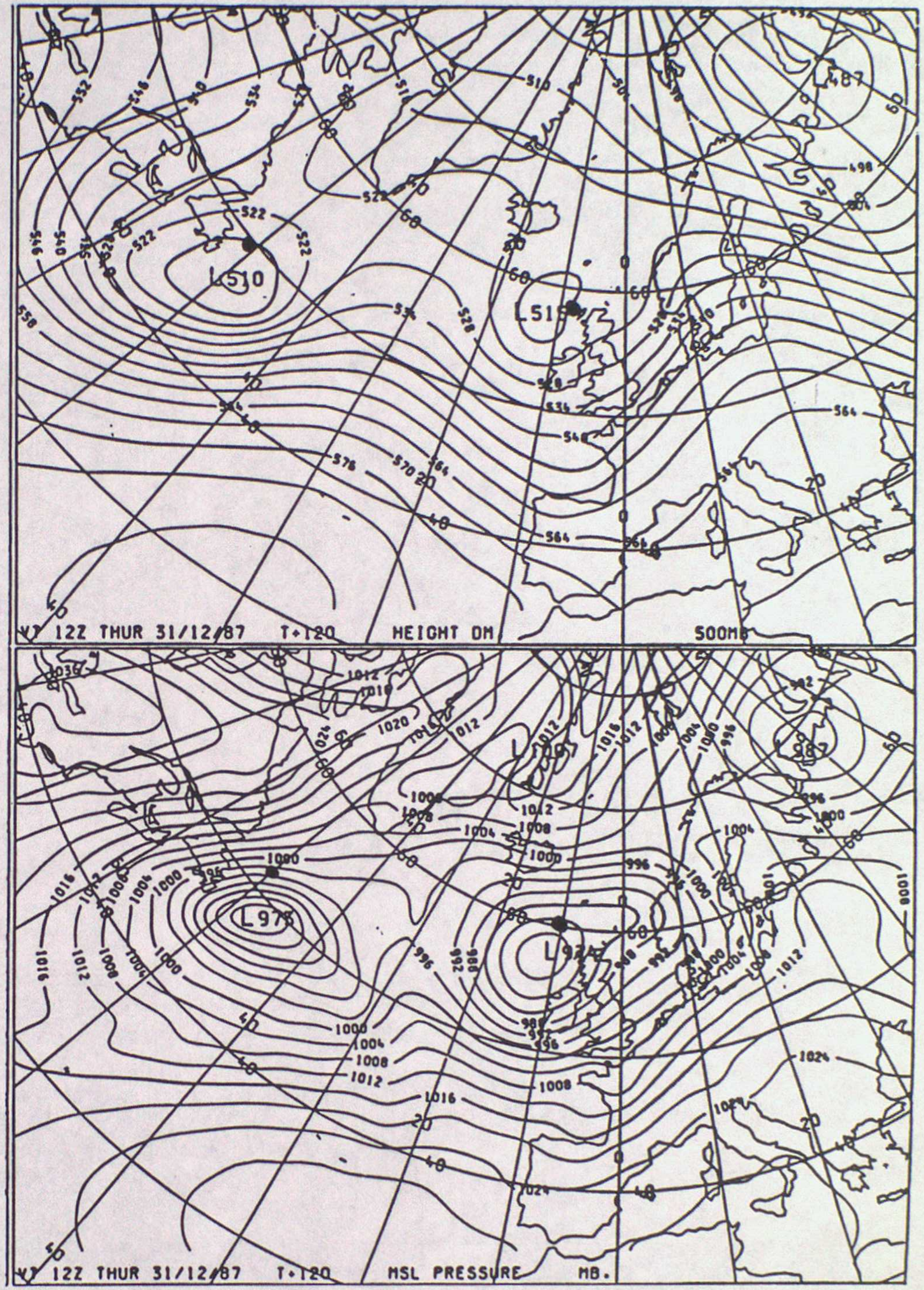

Figure 3 Operational forecast verifying against Figure 2.
Dots ● mark vortex centres on Figure 2.

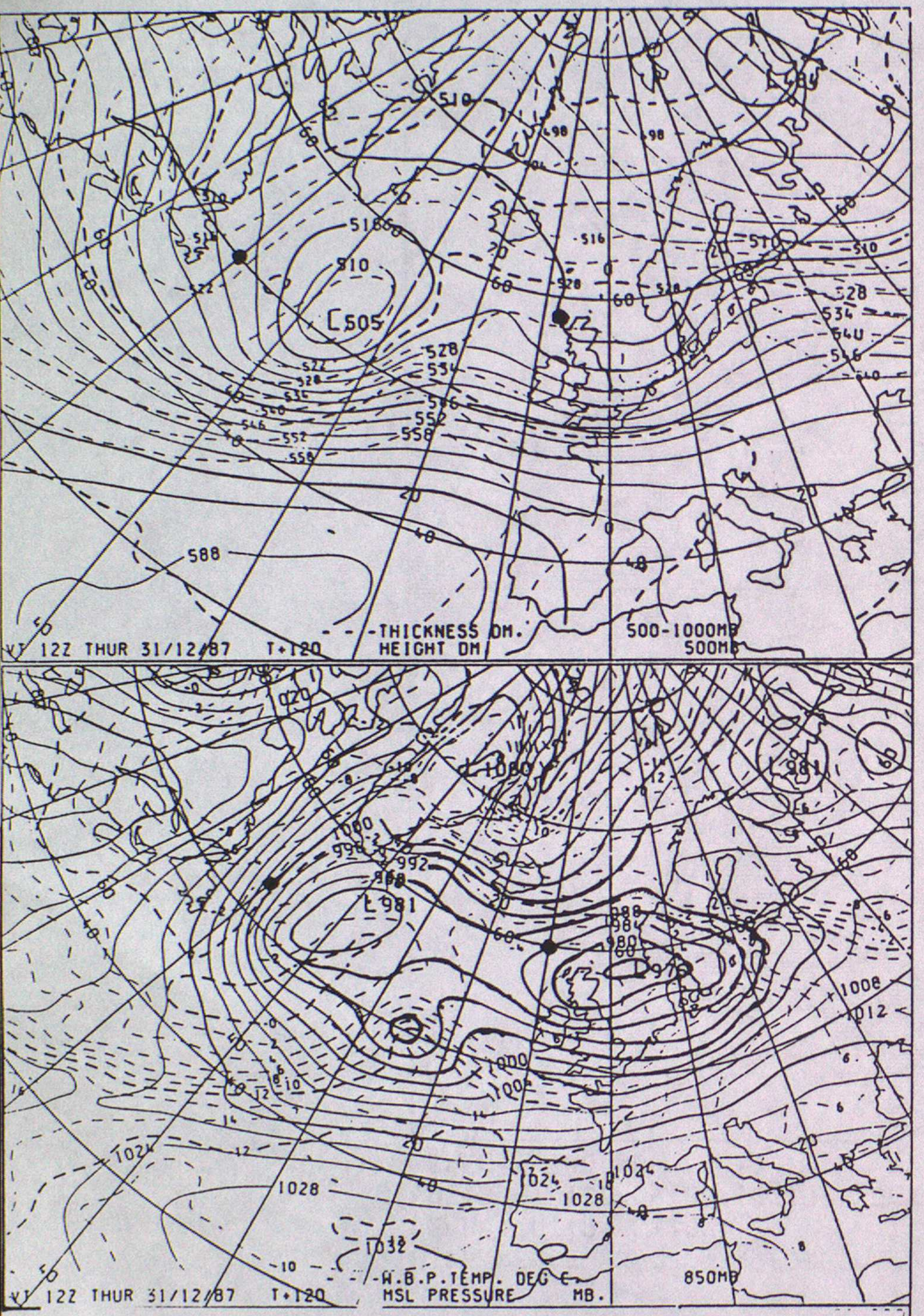

Figure 4 As Figure 3 for 5-day forecast from AC trial.

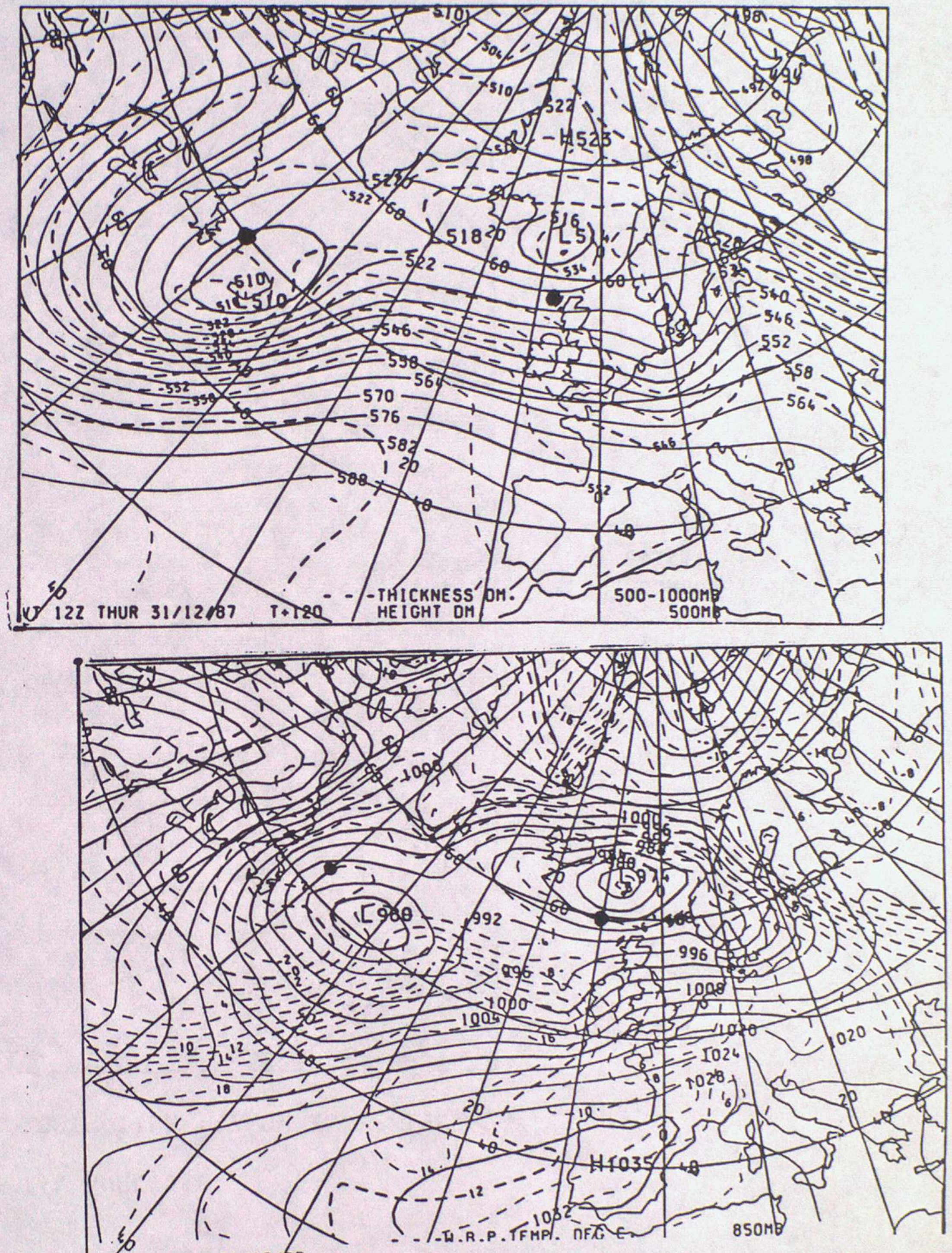

Figure 5 As Figure 3 for ECMWF 5-day forecast.

DIFFERENCE UK OP T+4 FORECAST - AC T+4 ANALYSIS
GEOPOTENTIAL HEIGHT
VALID AT 16Z ON 26/12/1987 DAY 360 DATA TIME 12Z ON 26/12/1987 DAY 360
LEVEL: 500 MB

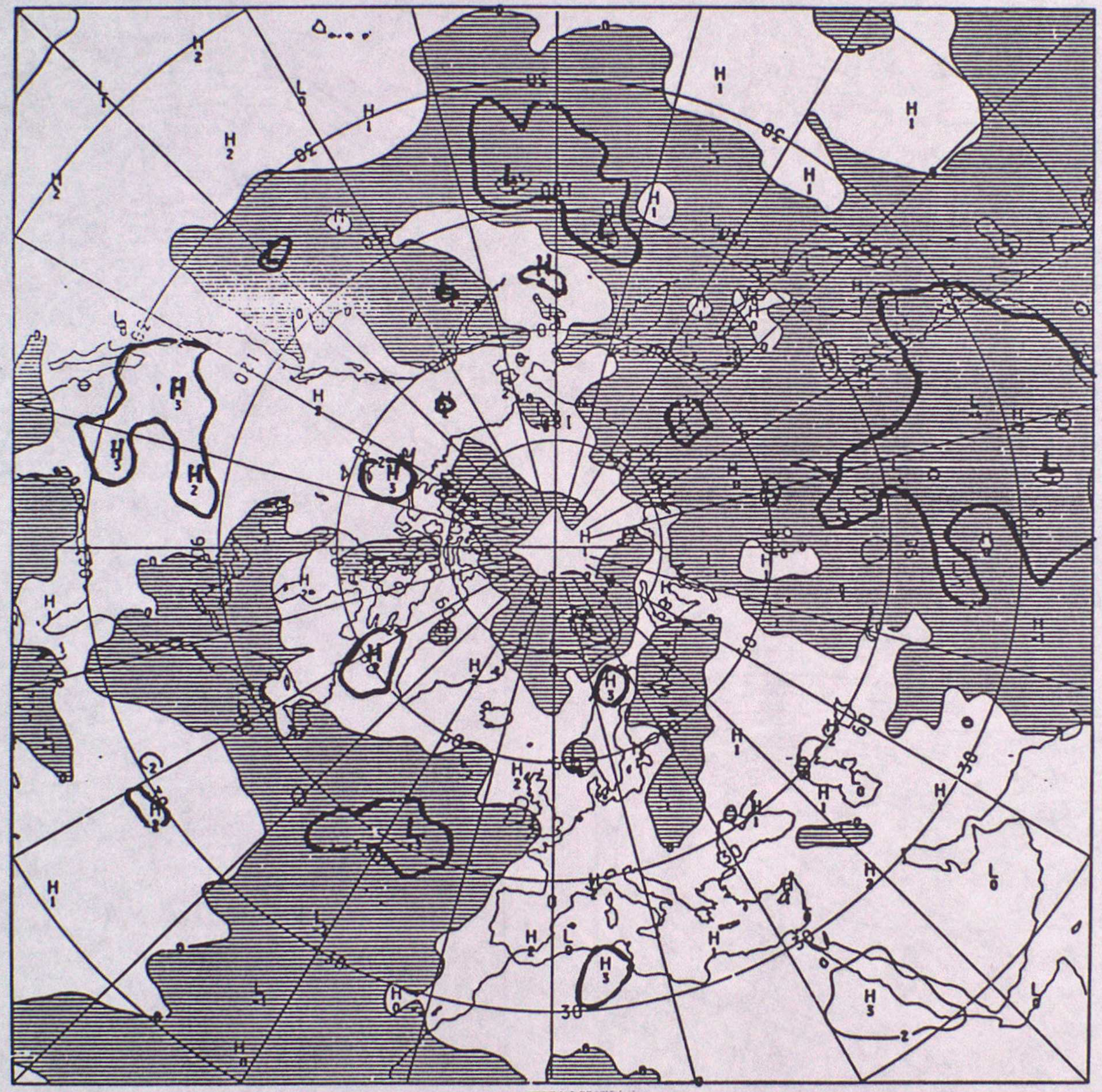

Figure 6

500mb height differences at t+4 between operational and AC trial runs (OP-AC).

DIFFERENCE UK OP FORECAST - AC T+4 ANALYSIS / UK FORECAST
GEOPOTENTIAL HEIGHT
VALID AT 12Z ON 31/12/1987 DAY 365 DATA TIME 12Z ON 26/12/1987
LEVEL: 500 MB

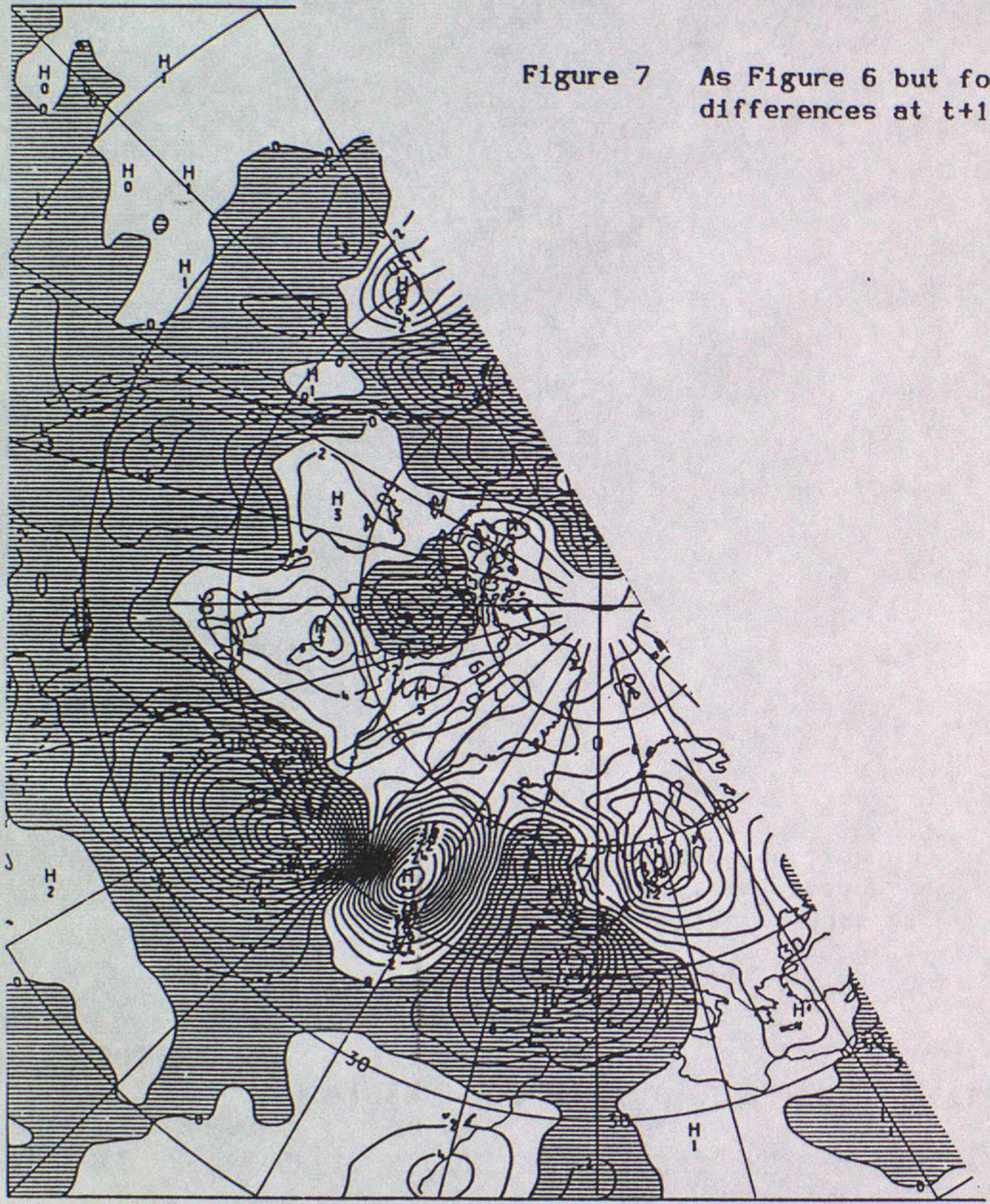

Figure 7 As Figure 6 but for differences at t+120.

DIFFERENCE AC T+4/OP TPLNT(20-70N, 90-140W)- AC T+4 ANAL
GEOPOTENTIAL HEIGHT
VALID AT 12Z ON 31/12/1987 DAY 365
LEVEL: 500 MB

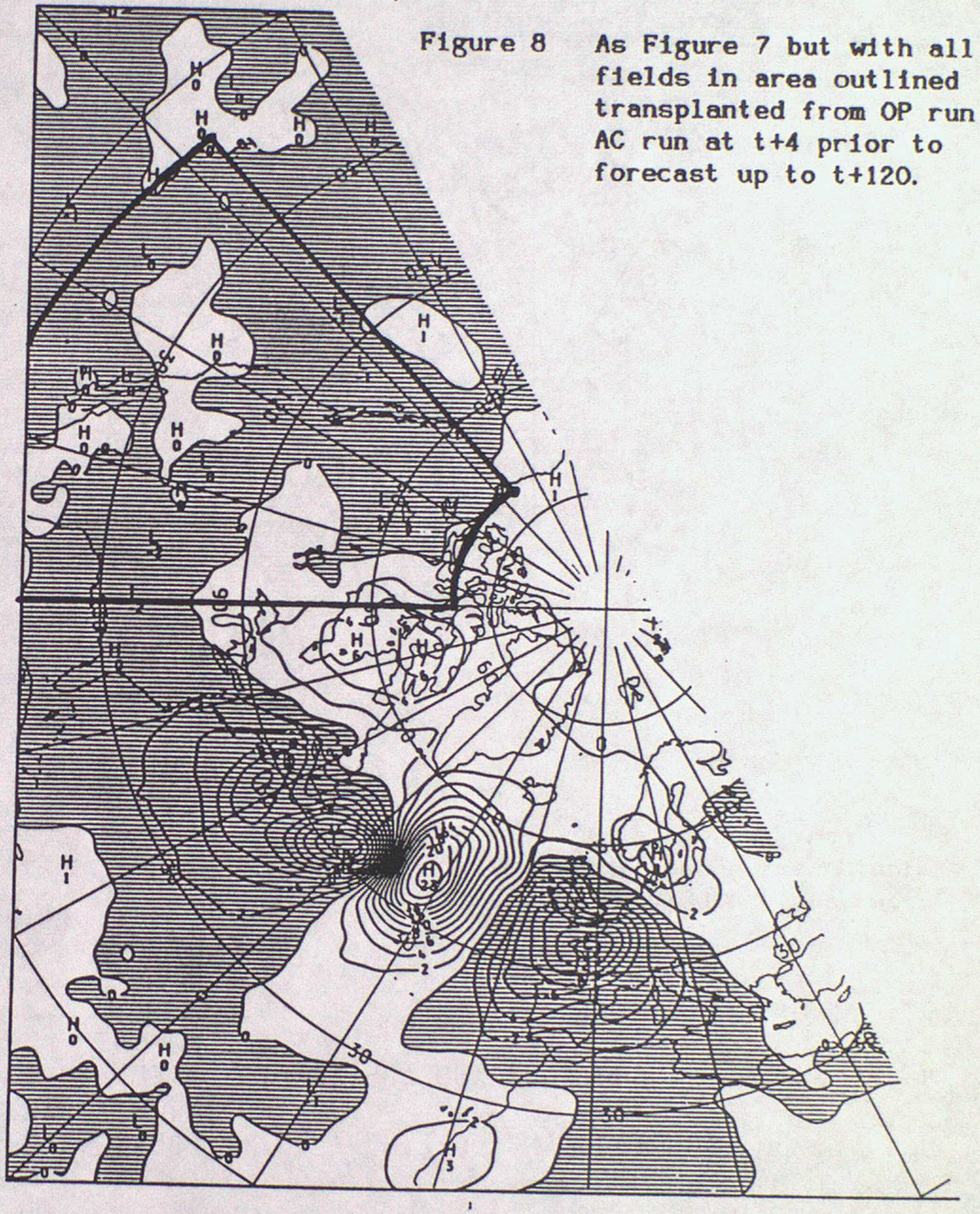

Figure 8 As Figure 7 but with all fields in area outlined transplanted from OP run t AC run at t+4 prior to forecast up to t+120.

IFFERENCE AC T+4/OP TPLNT(20-70N 90-120W)- AC T+4 ANAL
EOPOTENTIAL HEIGHT
ALID AT 12Z ON 31/12/1987 DAY 365 DATA TIME 12Z ON 26/12/1987
EVEL: 500 MB

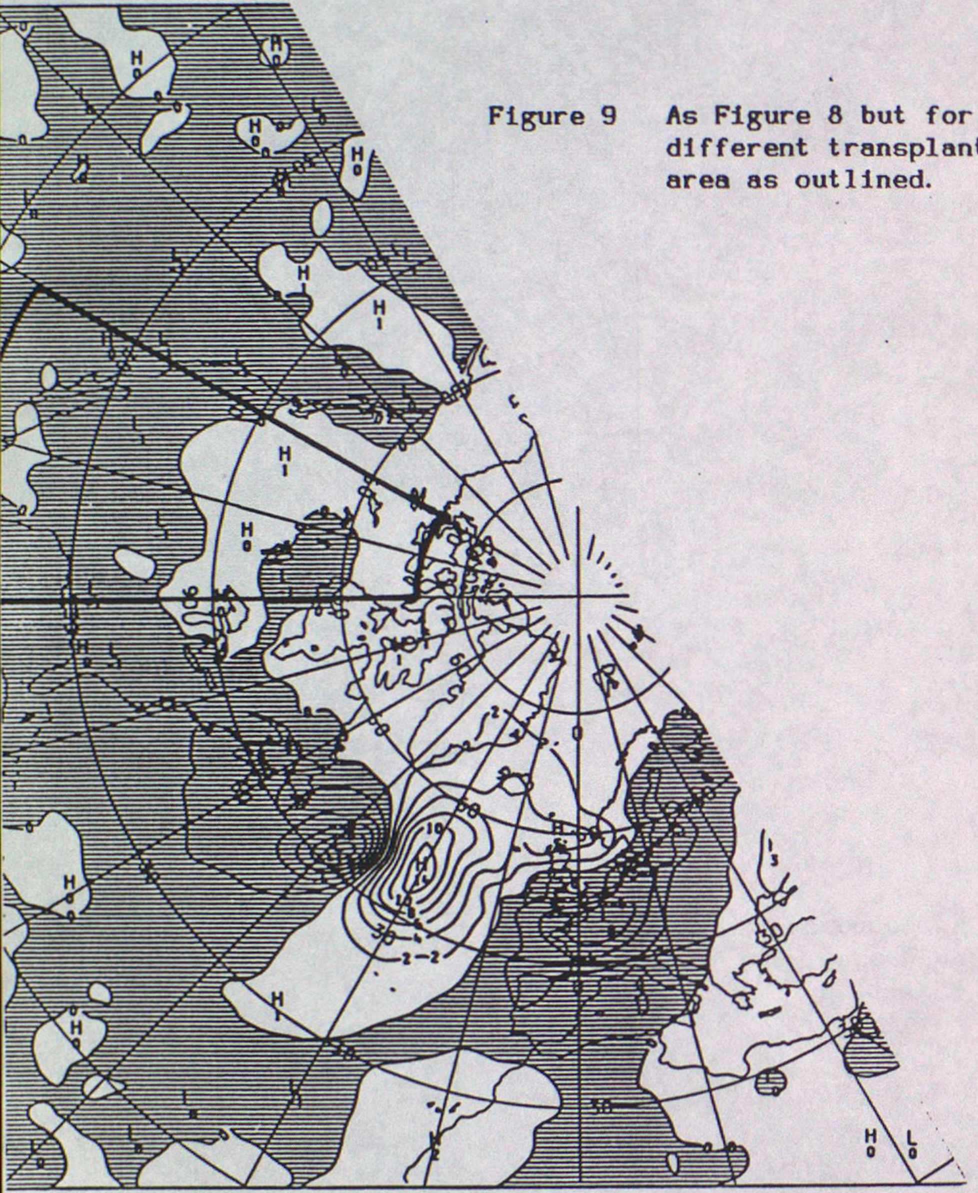

Figure 9 As Figure 8 but for different transplant area as outlined.

DIFFERENCE AC T+4/OP TPLNT(20-70N,120-150W)- AC T+4 ANAL
GEOPOTENTIAL HEIGHT
VALID AT 12Z ON 31/12/1987 DAY 365 DATA TIME 12Z ON 26/1
LEVEL: 500 MB

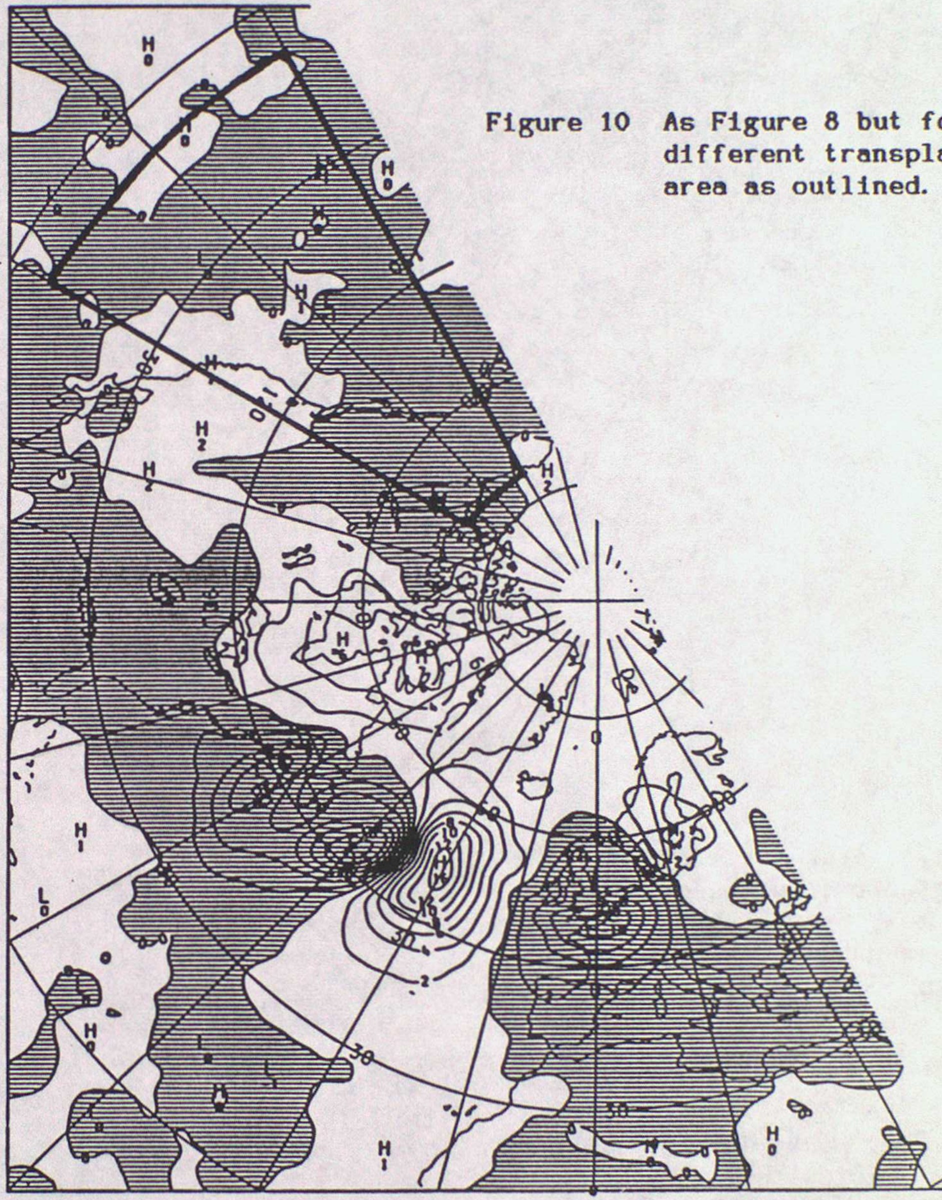

Figure 10 As Figure 8 but for different transplant area as outlined.

(a)

OP T+4
VALID AT 16Z ON 26/12/1987 DAY 360   DATA TIME 12Z ON 26/12/1987 DAY 360
LEVEL: 250 MB

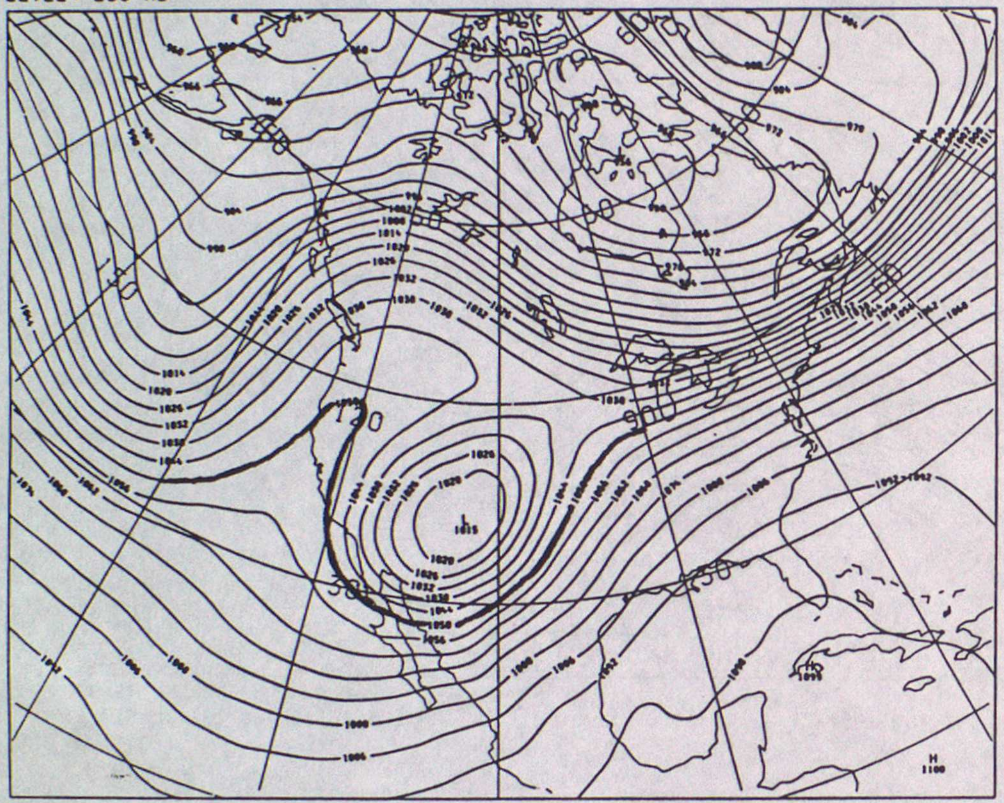

(b)

AC T+4
VALID AT 16Z ON 26/12/1987 DAY 360   DATA TIME 12Z ON 26/12/1987 DAY 360
LEVEL: 250 MB

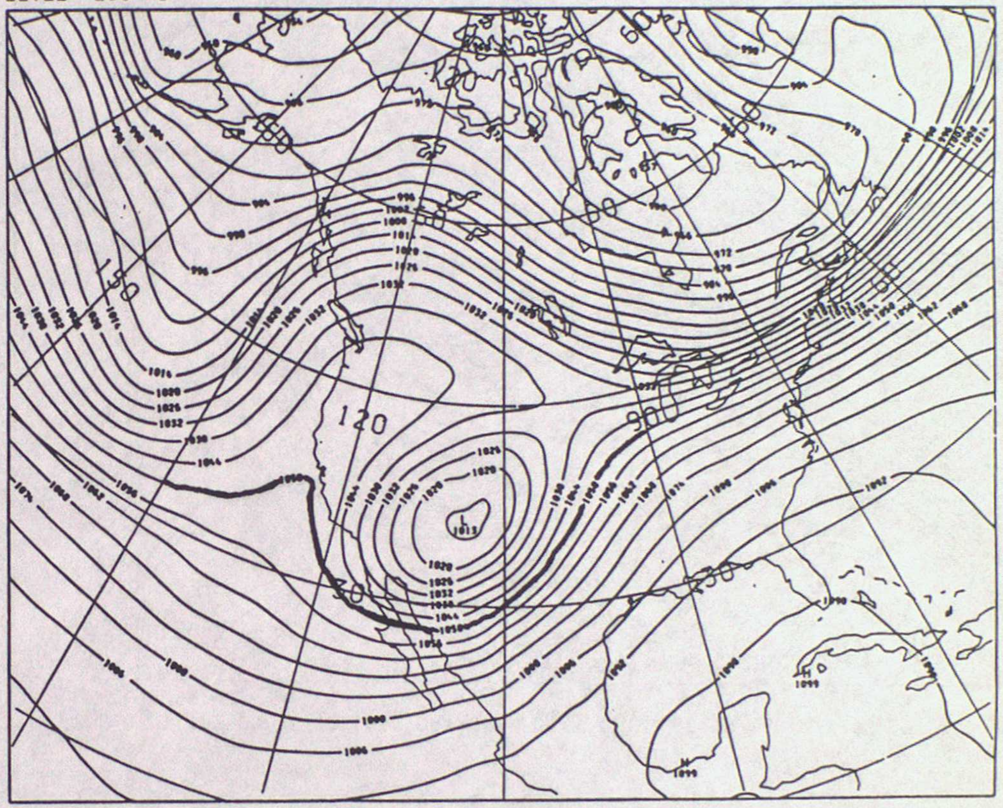

Figure 11 (a) Operational 250mb height field at t+4
(b) As (a) for AC trial run.

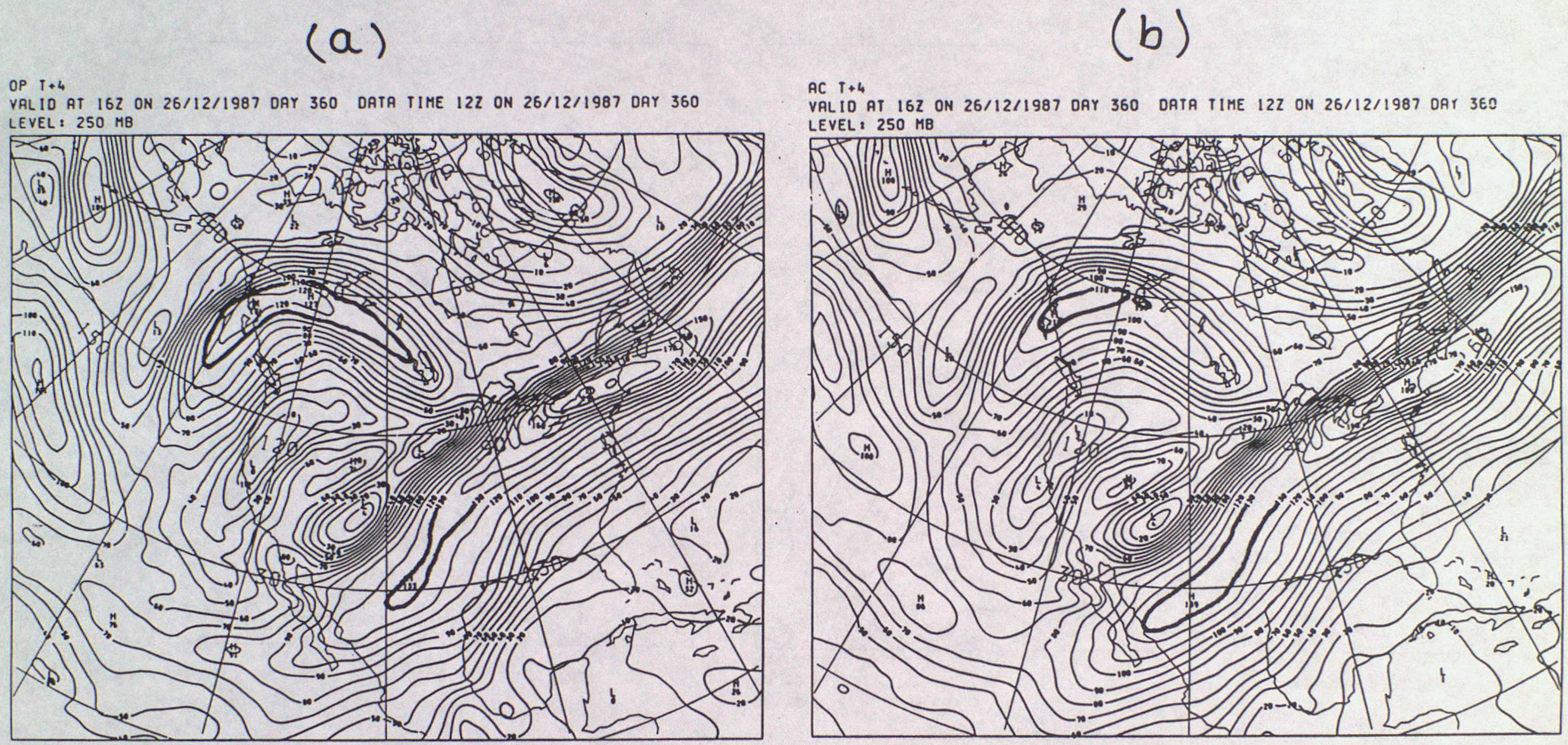

Figure 12 (a) Operational 250mb isotachs at t+4
(b) As (a) for AC trial run.

OP - AC T+4
VALID AT 16Z ON 26/12/1987 DAY 360 DATA TIME 12Z ON 26/12/1987 DAY 360
LEVEL: 250 MB

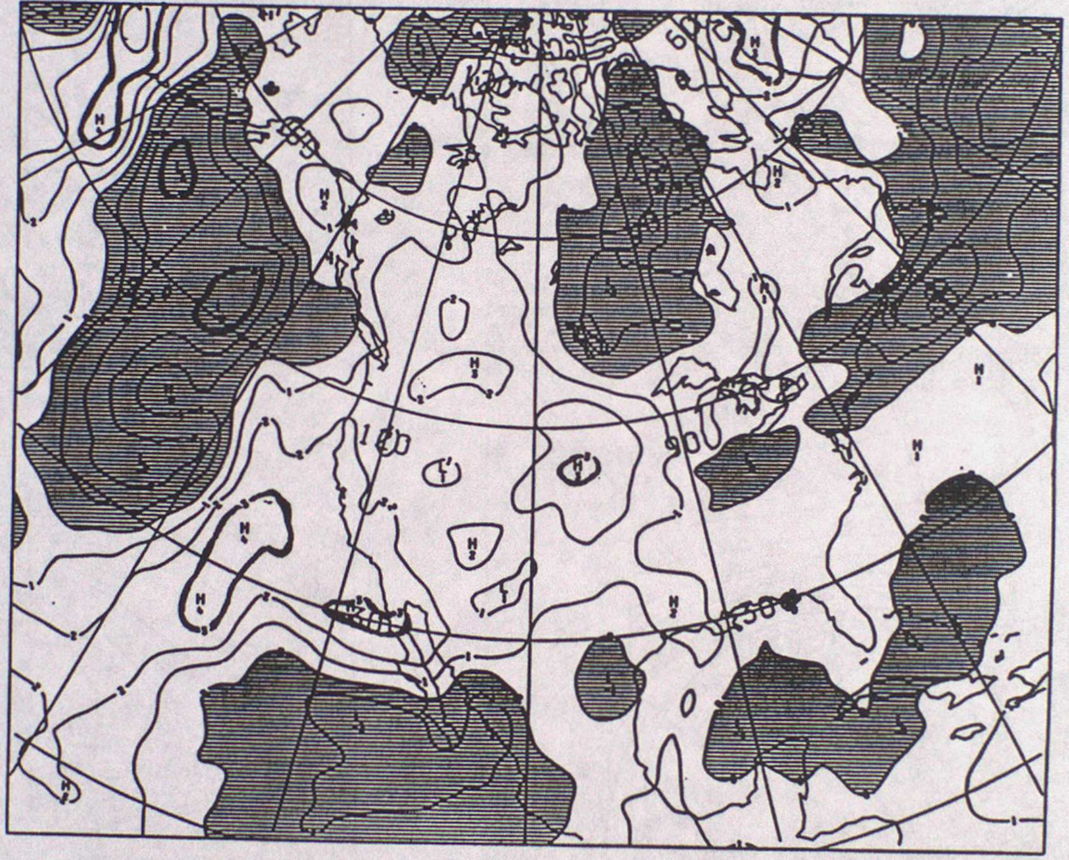

Figure 13 Differences in 250mb height at t+4 between operational and AC trial runs (OP-AC).

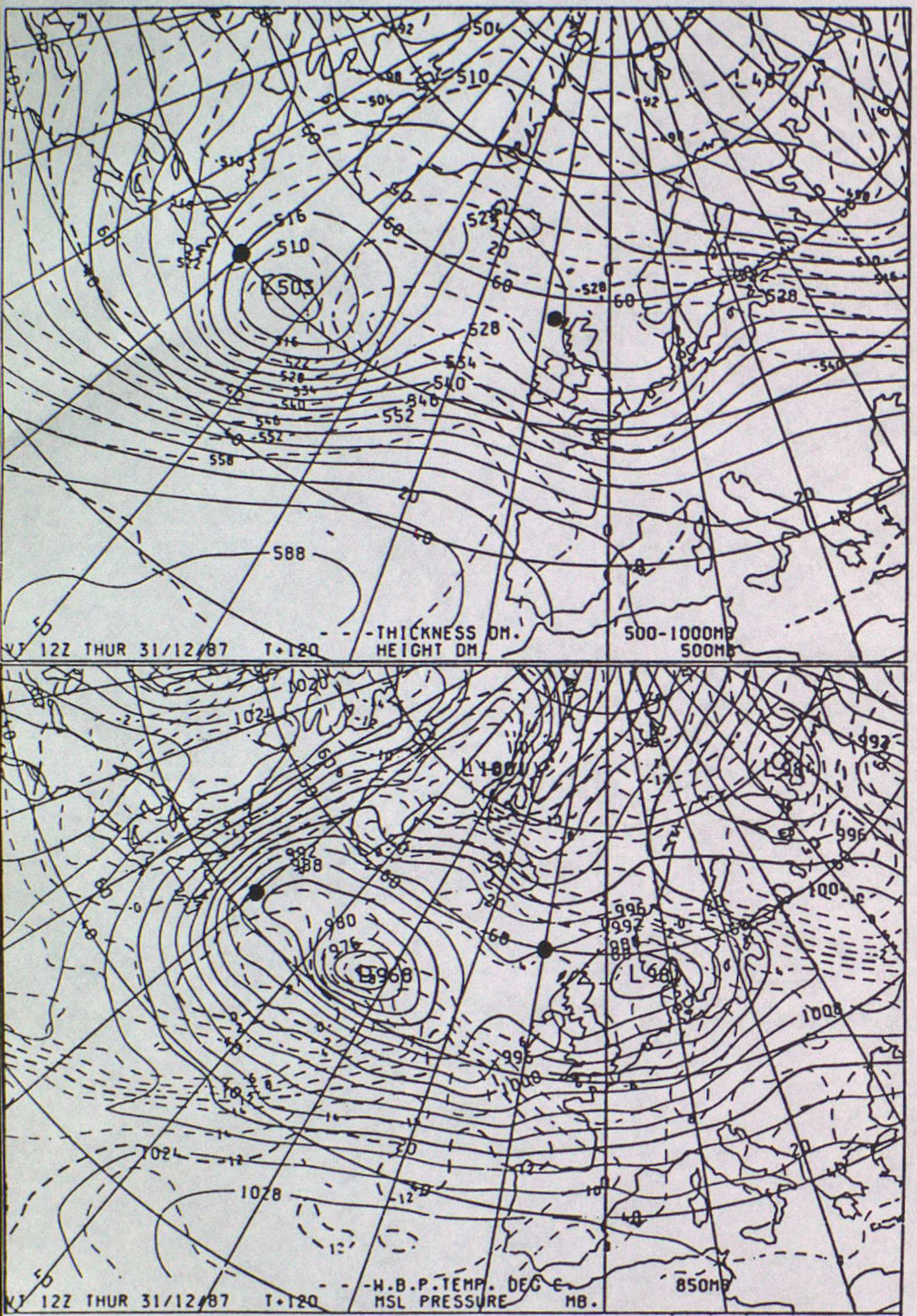

Figure 14 As Figure 4 but AC analysis remade by 24 hours of assimilation up to data time with a smaller influence area for radiosonde data.

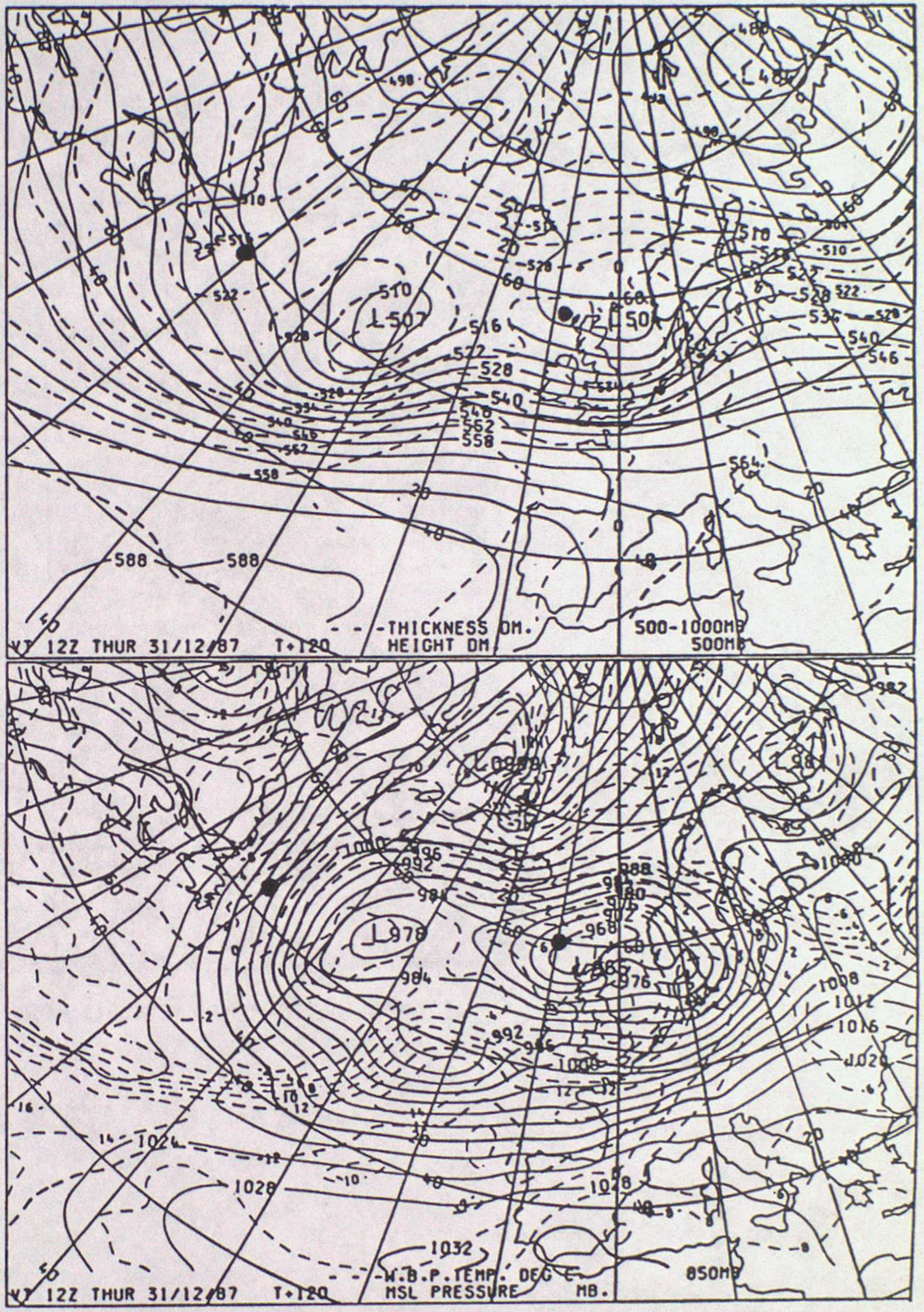

Figure 15 As Figure 4 but AC analysis remade by 24 hours of assimilation up to data time with a smaller influence area for airep and satob data.

EX4 - AC T+4
VALID AT 16Z ON 26/12/1987 DAY 360 DATA TIME 16Z ON 26/12/1987 DAY 360
LEVEL: 250 MB

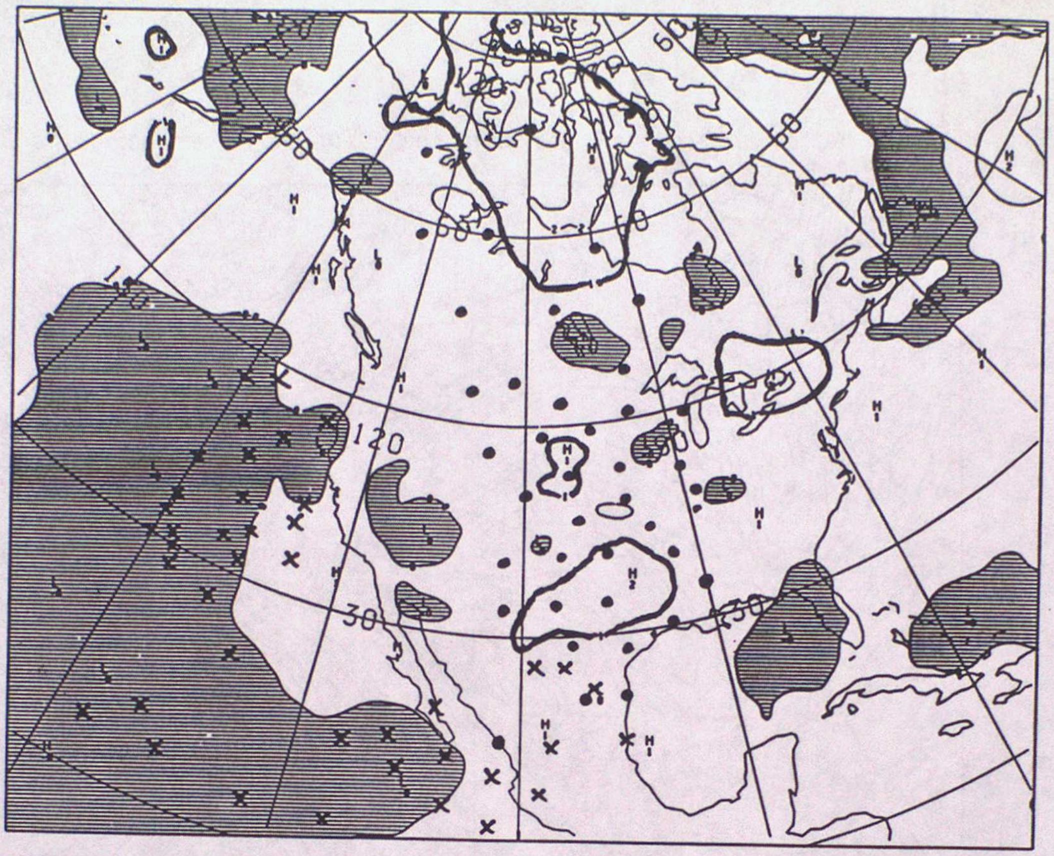

Figure 16 As Figure 13 but differences are for run with small radiosonde influence area - original AC trial run. Dots ● mark some radiosonde locations, crosses X mark airep and satob locations for the 12 GMT analysis on 26/12/87.

EX7 - AC T+4
VALID AT 16Z ON 26/12/1987 DAY 360 DATA TIME 16Z ON 26/12/1987 DAY 360
LEVEL: 250 MB

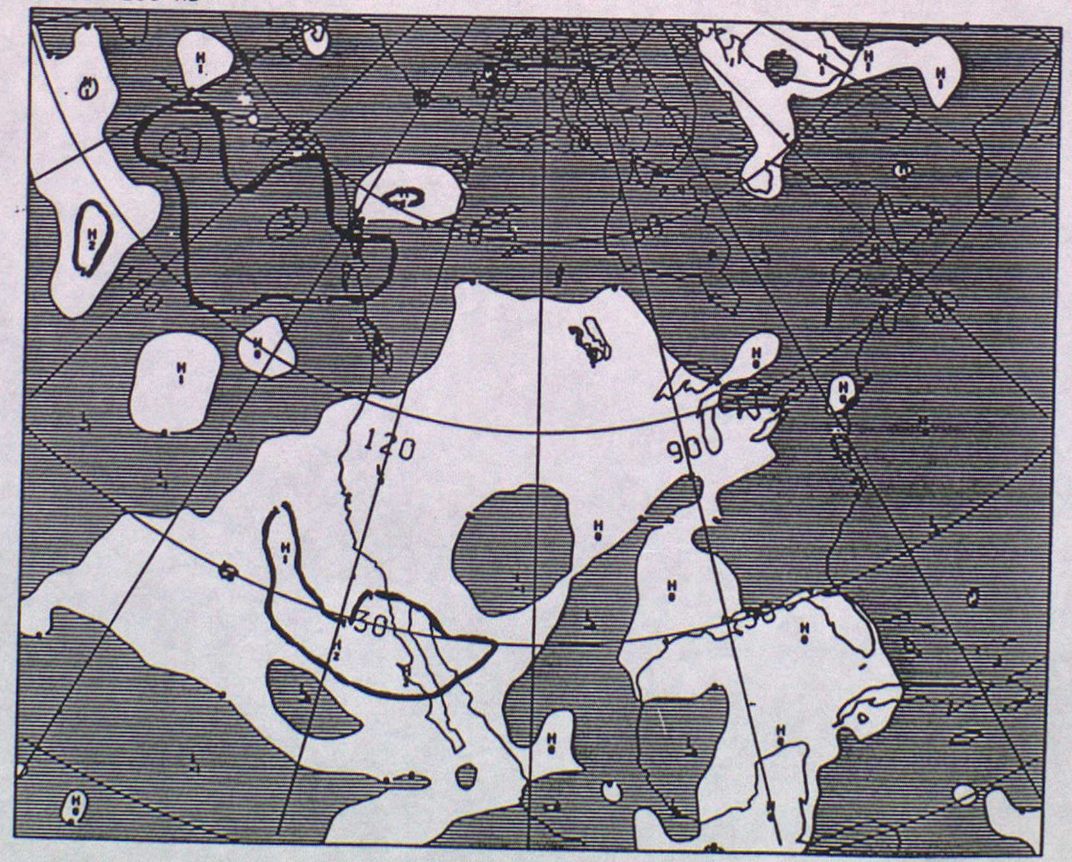

Figure 17 As Figure 16 but differences are for run with small influence area for airep and satob data - original AC trial run.

EX7 T+4
VALID AT 16Z ON 26/12/1987 DAY 360 DATA TIME 16Z ON 26/12/1987 DAY 360
LEVEL: 250 MB

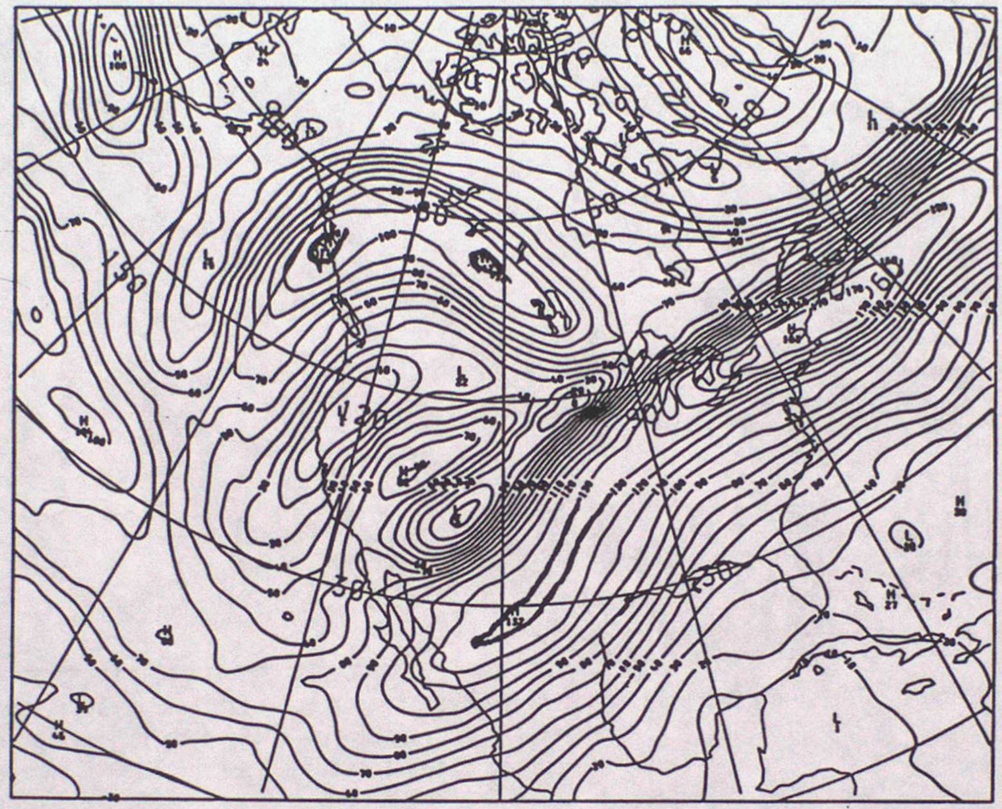

Figure 18 As Figure 12 but for AC run with smaller influence area for airep and satob data.

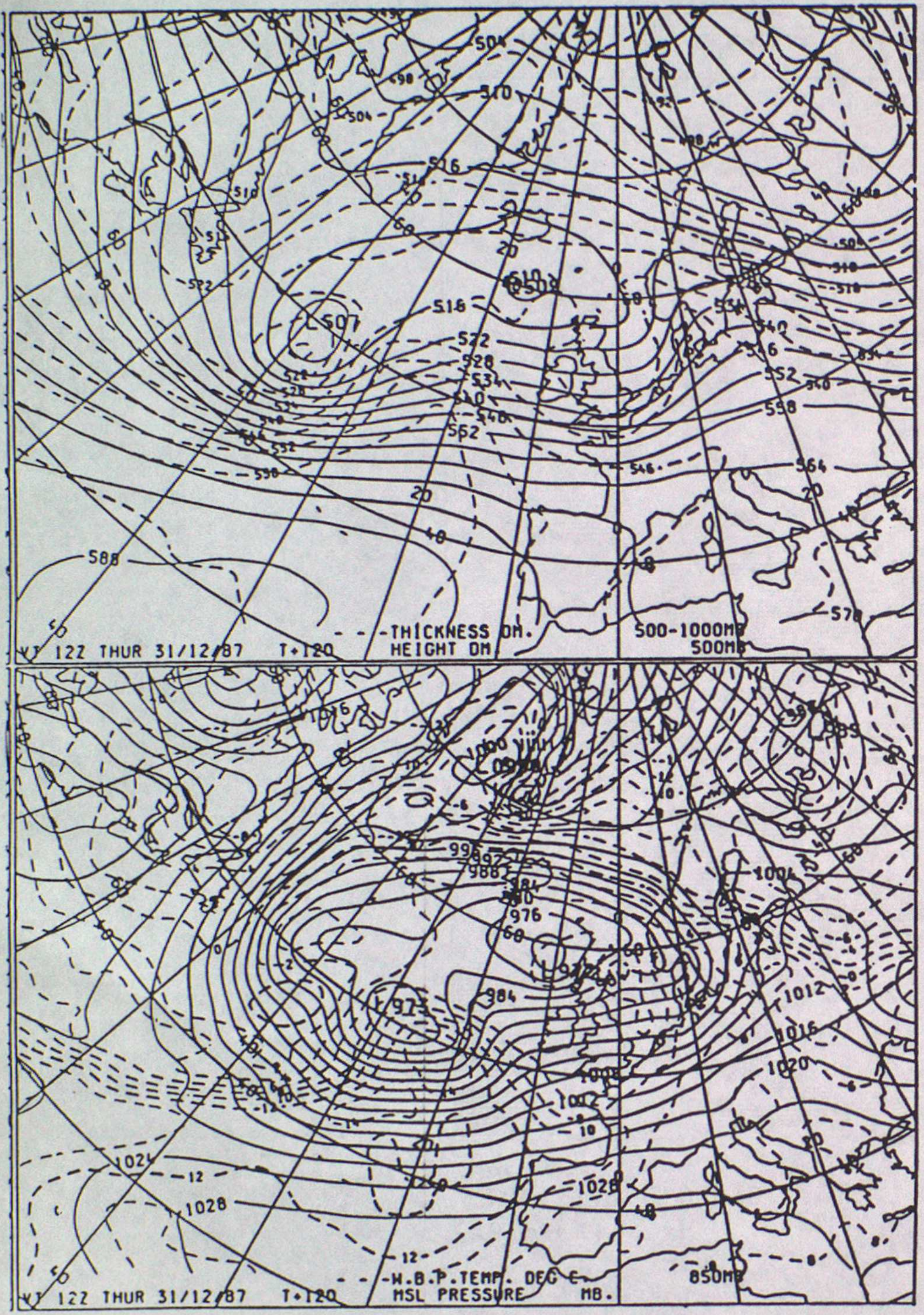

Figure 19 As Figure 4 for AC run with small influence area for all data.

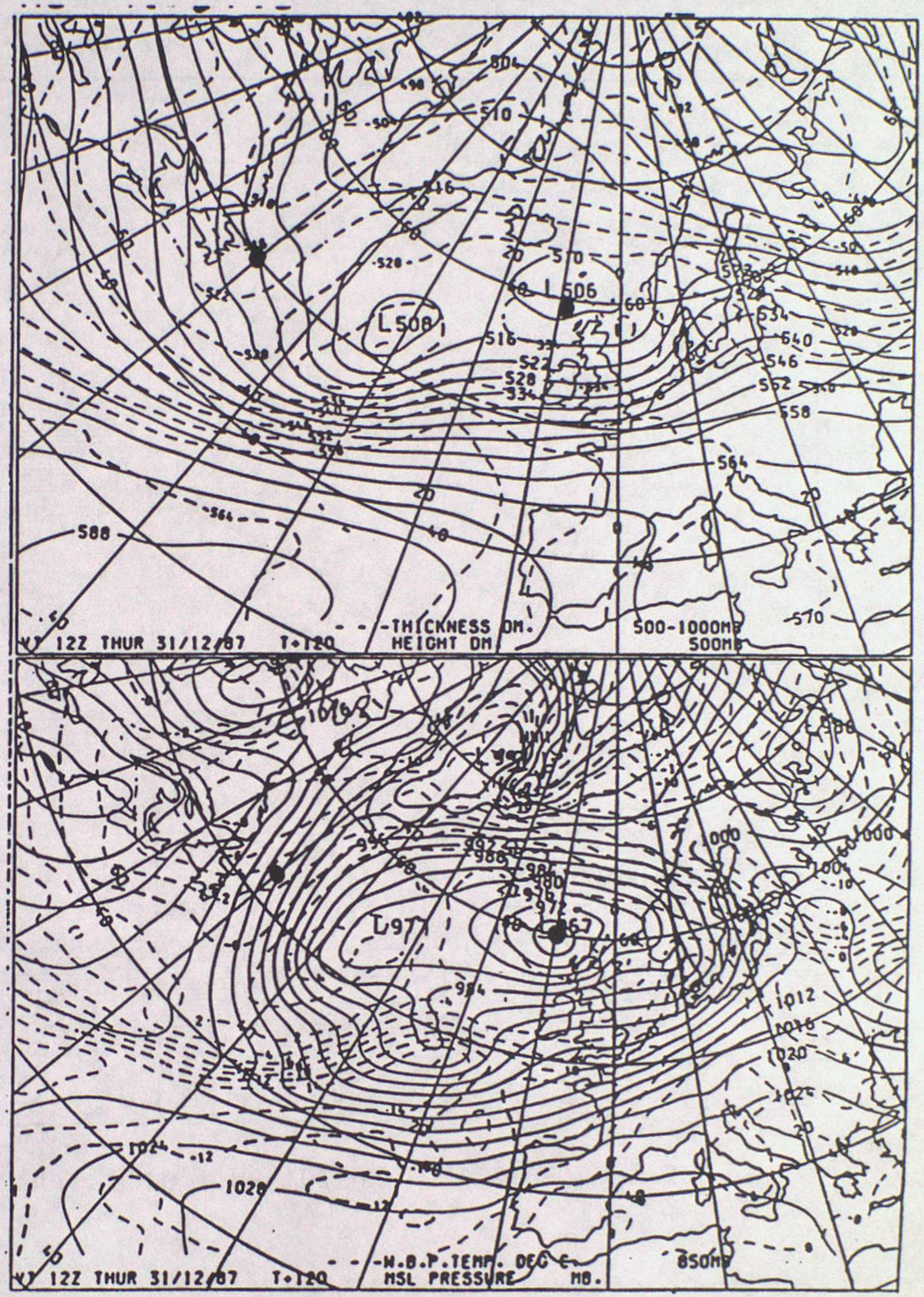

Figure 20 As Figure 19 but with reduced geostrophic coupling in the assimilation.

EX8 - EX19 T+4
VALID AT 16Z ON 26/12/1987 DAY 360 DATA TIME 16Z ON 26/12/1987 DAY 360
LEVEL: 250 MB

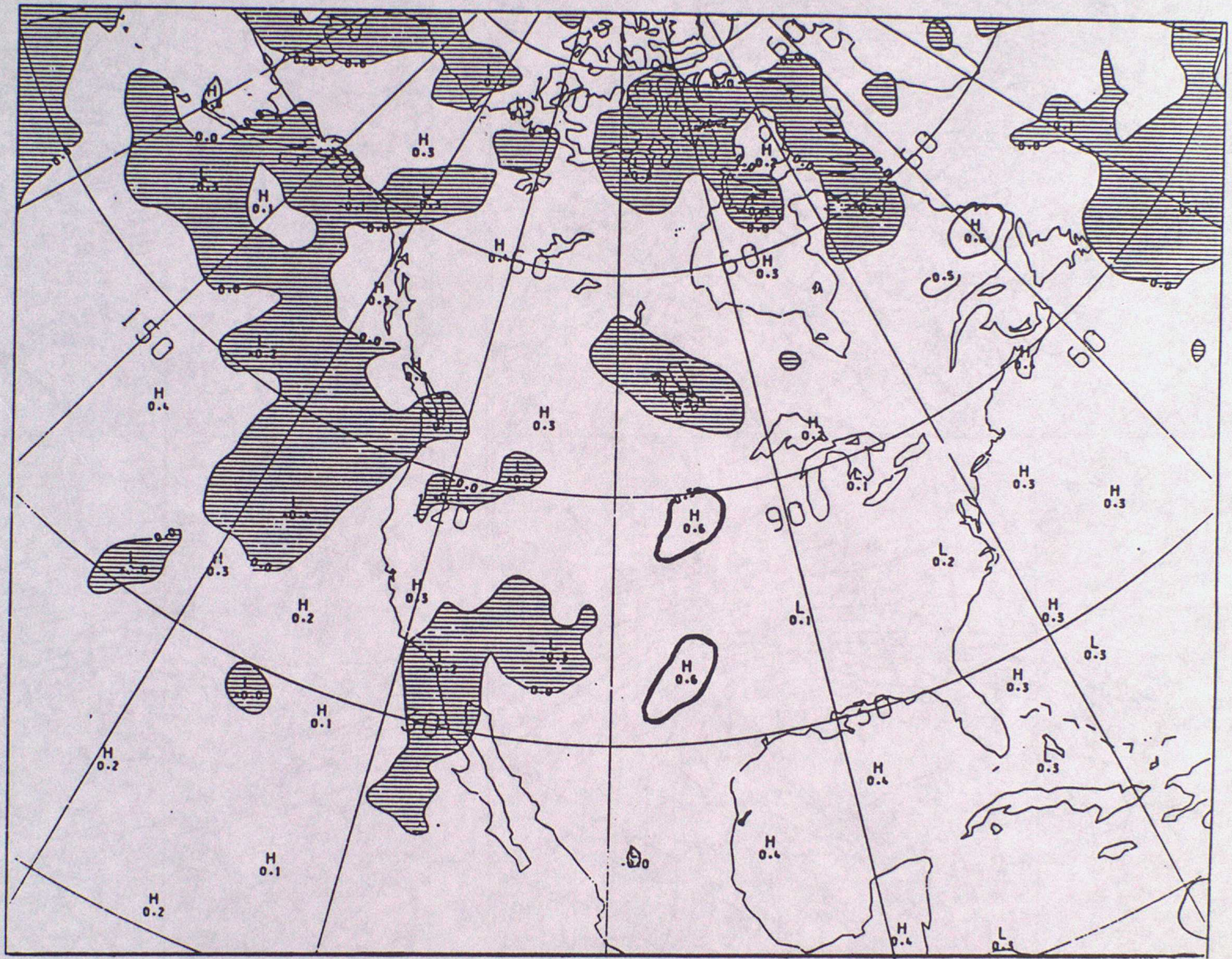

Figure 21 250mb height differences at t+4 for run in Figure 19 - run in Figure 20.

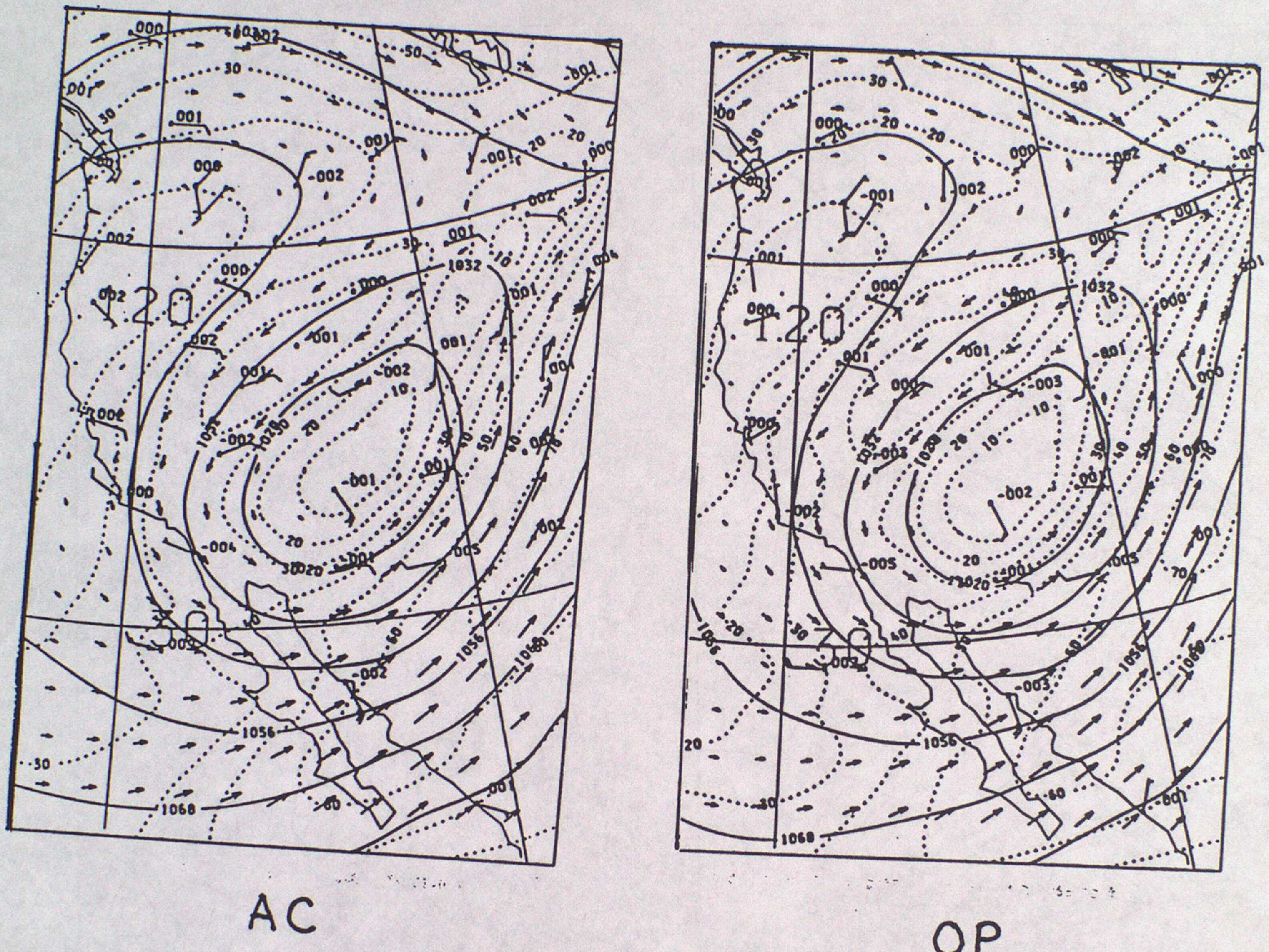

Figure 22 AC trial and OP 250 mb height fields (with isotachs dotted) at t+0 with height differences from verifying observations in dm and wind differences from observations in knots.

NO OF INFLUENCING OBS/GRID PT - OPERATIONAL AC RNX=3.5
SCALE=300KM. TIME FACTOR=1 . WIND OBS
VALIDITY TIME : 1200Z 26/12/1987 TIMESTEP NO. 1
LEVEL: SIGMA=0.250

Figure 23 Number of influencing observations per grid point for wind data at 250mb in AC trial run.

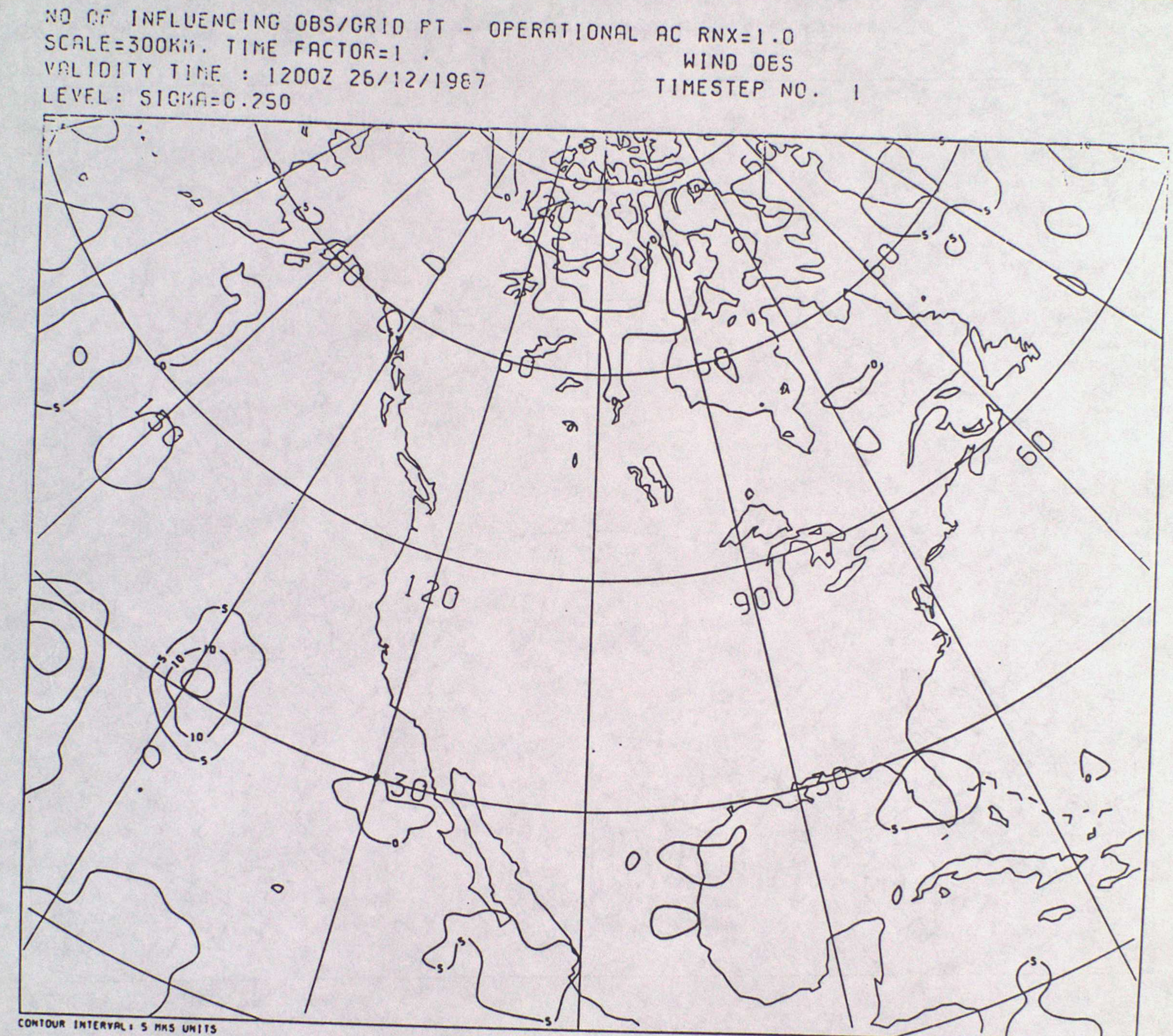

Figure 24 As Figure 23 for AC run with small influence area for all data.

NO OF INFLUENCING OBS/GRID PT - VARIABLE INFLUENCE RAD
SCALE=300KM. TIME FACTOR=1 . WIND OBS
VALIDITY TIME : 1200Z 26/12/1987 TIMESTEP NO. 1
LEVEL: SIGMA=0.250

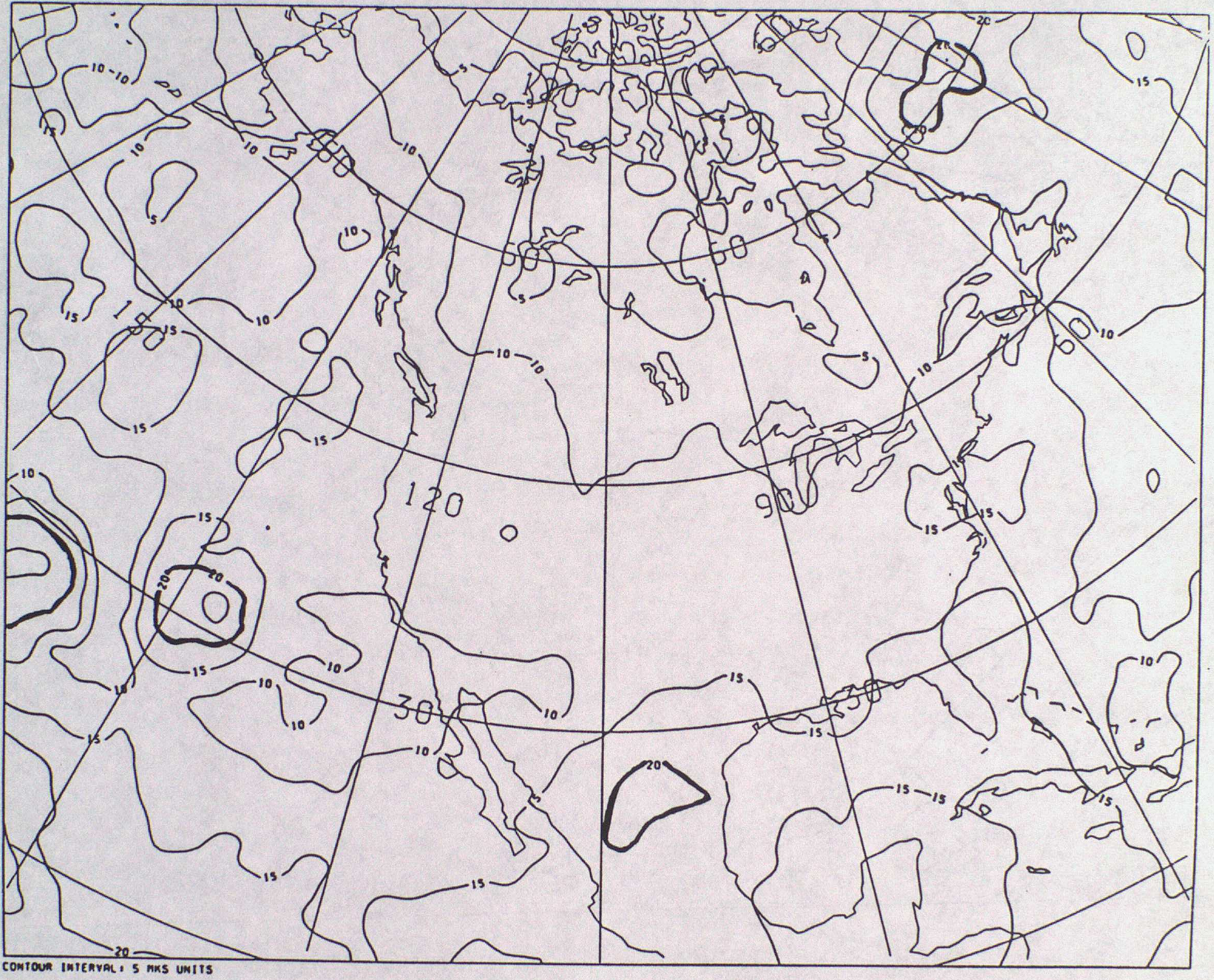

Figure 25 As Figure 23 for AC run with variable influence area scheme described in Section 5.

SUM OF NORMALISED WEIGHTS - OPERATIONAL AC RNX=3.5
SCALE=300KM. TIME FACTOR=1 . WIND OBS
VALIDITY TIME : 1200Z 26/12/1987 TIMESTEP NO. 1
LEVEL: SIGMA=0.250

Figure 26 Sum of normalised weights at each grid point (see equation (5.9)) for wind data at 250mb in original AC trial run. The 1·0 contour is highlighted.

SUM OF NORMALISED WEIGHTS - VARIABLE INF RADIUS
SCALE=300KM. TIME FACTOR=1 . NO RENORM WIND OBS
VALIDITY TIME : 1200Z 26/12/1987 TIMESTEP NO. 1
LEVEL: SIGMA=0.250

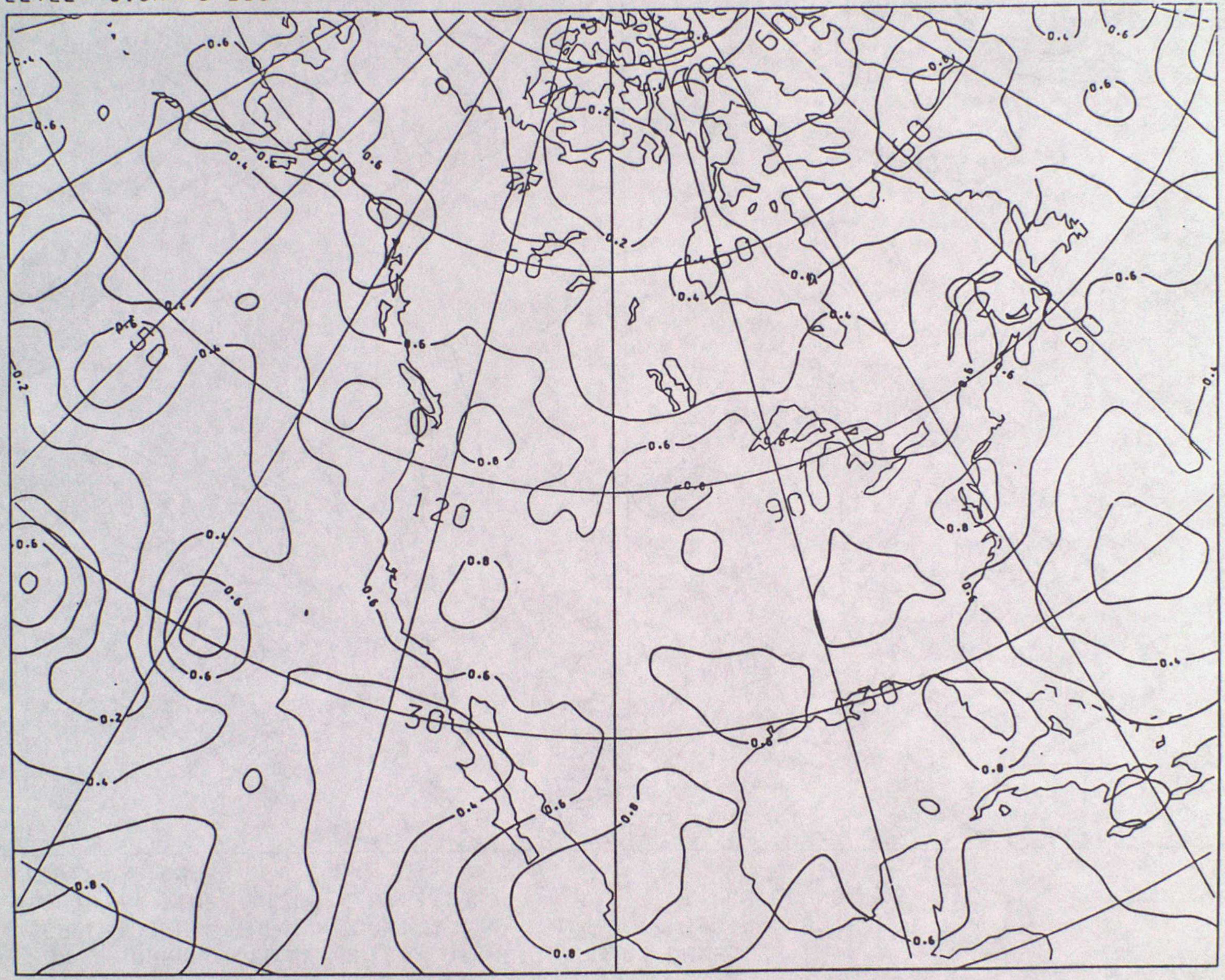

Figure 27 As Figure 26 for variable influence area scheme with *no* weights renormalisation.

SUM OF NORMALISED WEIGHTS - VARIABLE INF RADIUS
SCALE=300KM. TIME FACTOR=1 . WIND OBS
VALIDITY TIME : 1200Z 26/12/1987 TIMESTEP NO. 1
LEVEL: SIGMA=0.250

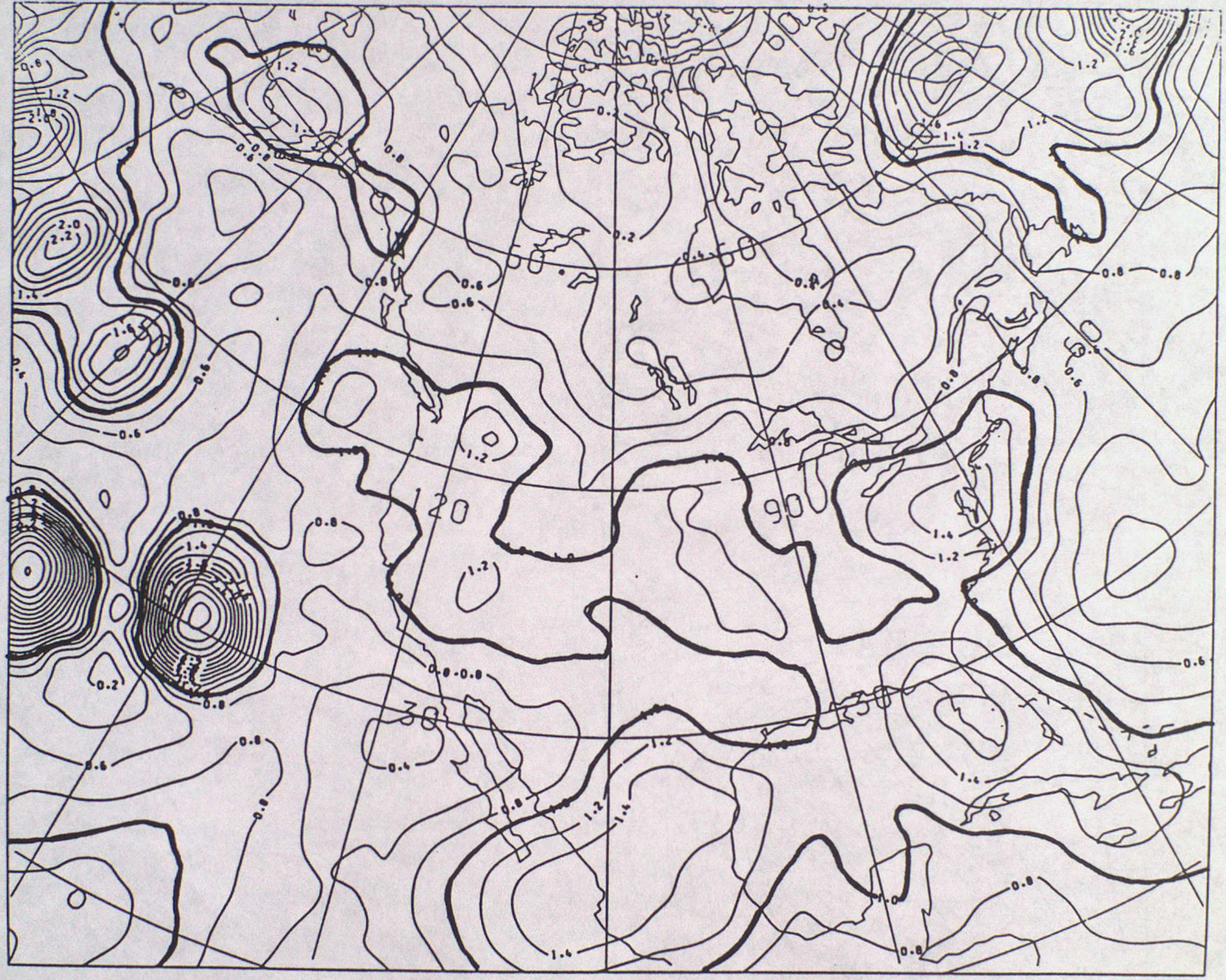

Figure 28 As Figure 27 *with* weights renormalisation.

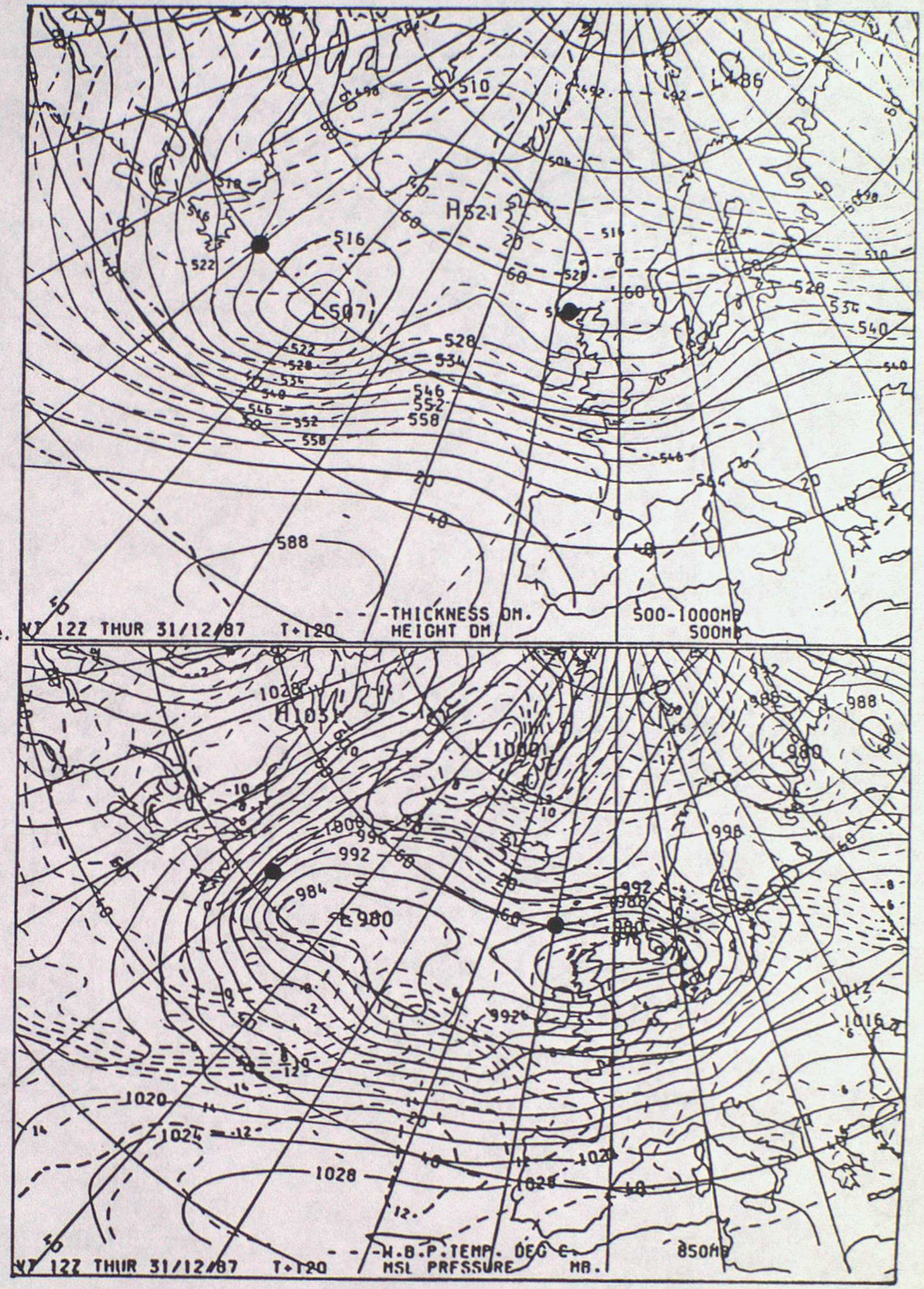

Figure 29 As Figure 4 for AC run with variable influence area scheme.

Recent Met O 11 Technical Notes (New Series)

15. The sensitivity of a medium range forecast with the analysis correction scheme to data selection in the horizontal.
B. Macpherson and R.A. Downton
November 1989

16. The sensitivity of fine-mesh rainfall forecasts to changes in the initial moisture fields.
R.S. Bell and O.M. Hammon
August 1988

17. Conservative finite difference schemes for a unified forecast/climate model.
M.J.P. Cullen and T. Davies
July 1988

18. Interpreting results from numerical models.
T. Davies
August 1988

19. A comparison of the OWSE assimilation scheme with the operational global assimilation scheme.
D.N. Reed and M.A. Ayles
October 1988

20. Improvements to low cloud forecasts from the mesoscale and fine mesh models.
O.M. Hammon
October 1988

21. The effect of route choice on aircraft wind observations over the North Atlantic.
D. Long and N.B. Ingleby
October 1988

22. Maximum liklihood de-aliasing of simulated scatterometer wind fields using adaptive descent algorithms.
R.J. Purser
January 1989

23. A proposal for assimilating detailed aircraft wind data in a local area.
R.J. Purser
January 1989

24. Basic formulation and boundary conditions of the mesoscale model.
S.P. Ballard
Not yet issued.

25. Development of a new physics package for the global forecast model.
C.A. Wilson and J. Slingo
January 1989

Recent Met O 11 Technical Notes (New Series)

26.	The trial of the fine-mesh version of the analysis correction scheme	O. M. Hammon R. A. Bromley B. Macpherson May 1989
27.	The New Meteorological Office Data Assimilation Scheme	A. C. Lorenc R. S. Bell B. Macpherson April 1989
28.	Model error structure and estimated analysis accuracy with a network of wind profilers	N. B. Ingleby R. A. Bromley April 1989
29.	Examples of hybrid vertical co-ordinate systems for the unified forecast/climate model.	R. Swinbank July 1989
30.	The Meteorological Office Experimental Mesoscale Numerical Weather Prediction System: July 1989	B. W. Golding July 1989
31.	Tests of the Heun Advection Scheme.	B. L. Marshall July 1989
32.	Not Yet Available	R. A. Bromley R. A. Downton
33.	Spatial diagnostics of operational assimiliations using the observation processing database.	P. Jemmer August 1989
34.	Enhancements to the Mesoscale Model and their impact on forecasts.	S. P. Ballard September 1989
35.	Preliminary stratospheric analysis experiments with the Analysis Correction scheme.	R. Swinbank October 1989
36.	A diagnostic study of the impact of Seasat scatterometer winds on numerical weather prediction.	N. B. Ingleby R. A. Bromley October 1989
37.	Extension of the Bayesian Ship Quality Control Scheme to all Surface Data, and a trial of the Quality Control of Land Synops.	C. A. Parrett O. M. Hammon November 1989
38.	The impact of satellite sounding data in the fine-mesh model.	R. S. Bell O. M. Hammon December 1989
39	NWP systems of the future at the UK Meteorological Office, and the likely impact of windprofiler observations.	A. C. Lorenc November 1988
40	The Impact of the Interactive Mesoscale Initialisation	B. J. Wright B. W. Golding November 1989